University of Pennsylvania
ScholarlyCommons

Publicly Accessible Penn Dissertations

2017

R-Spondin-2 Modulates Osteoblastogenesis And Bone Accrual

Meghan Noelle Knight
University of Pennsylvania, mkni@vet.upenn.edu

R-Spondin-2 Modulates Osteoblastogenesis And Bone Accrual

Abstract

The R-spondin family of proteins are Wnt agonists, and the complete embryonic disruption of Rspo2 results in skeletal developmental defects that recapitulate the phenotype observed with Lrp5/6 deficiency. Previous work has shown that Rspo2 is both highly expressed in Wnt stimulated pre-osteoblasts and that its over-expression induces osteoblast differentiation in the same cells, supporting its role as a positive autocrine regulator of osteoblastogenesis. However, the role of Rspo2 in the autocrine regulation of osteoblastogenesis in postnatal bone is under explored. Here, we show that limb-bud progenitor cells from Rspo2 knockout mice undergo reduced mineralization during osteoblastogenesis in vitro, and have a corresponding alteration in their osteogenic gene expression profile. The first Rspo2 conditional knockout (Rspo2floxed) mouse was generated, and Rspo2 was knocked out in osteoblasts by crossing to the OsteocalcinCre mouse line (Ocn-Cre+ Rspo2f/f) to address the autocrine role of Rspo2 in vivo. OcnCre+Rspo2f/f male and female mice at 1, 3, and 6 months were examined. Ocn-Cre+Rspo2f/f mice are decreased in overall body size compared to their littermates, and they have decreased trabecular bone mass due primarily to decreased trabecular thickness. Histomorphometric analysis revealed a similar number of osteoblasts and mineralizing surface per bone surface with a simultaneous decrease in mineral apposition and bone formation rates, suggesting that a decreased mineralization capacity rather than an overall reduced number of osteoblasts is the etiology of the reduced bone volume. In following with this, BM-MSC from Ocn-Cre+Rspo2f/f mice undergo less mineralization in vitro. Overall, Rspo2 loss reduces osteoblastogenesis and mineralization both in vitro and in vivo, leading to reduced bone mass.

Degree Type
Dissertation

Degree Name
Doctor of Philosophy (PhD)

Graduate Group
Cell & Molecular Biology

First Advisor
Jaimo Ahn

Second Advisor
Kurt D. Hankenson

Subject Categories
Cell Biology | Developmental Biology

R-SPONDIN-2 MODULATES OSTEOBLASTOGENESIS AND BONE ACCRUAL

Meghan Noelle Knight

A DISSERTATION

in

Cell and Molecular Biology

Presented to the Faculties of the University of Pennsylvania

in

Partial Fulfillment of the Requirements for the

Degree of Doctor of Philosophy

2017

Supervisor of Dissertation

_____

Jaimo Ahn, M.D., Ph.D.

Assistant Professor of Orthopaedic Surgery

Co-Supervisor of Dissertation

_____

Kurt D. Hankenson, D.V.M., M.S., Ph.D.

Professor of Orthopaedic Surgery,

University of Michigan

Graduate Group Chairperson

_____

Daniel S. Kessler, Ph.D.

Associate Professor of Cell and Developmental Biology

Dissertation Committee

Sarah E. Millar, Ph.D. Albert M. Kligman Professor in Dermatology

Maurizio Pacifici, Ph.D. Professor of Orthopaedic Surgery

Struan F.A. Grant, Ph.D. Associate Professor of Pediatrics

Foteini Mourkioti, Ph.D. Assistant Professor of Orthopaedic Surgery

R-SPONDIN-2 MODULATES OSTEOBLASTOGENESIS AND BONE ACCRUAL THROUGH

WNT SIGNALING

COPYRIGHT

2017

Meghan Noelle Knight

For Joy.

November 30, 1978 – April 5, 2005

iii

ACKNOWLEDGMENTS

In order to complete this dissertation, I have truly had to stand on the shoulders of giants. First, and foremost, I would like to thank my advisors, Dr. Kurt Hankenson and Dr. Jaimo Ahn. They have been incredible mentors: fostering my scientific growth, encouraging me and helping to clear any obstacles in my path, and perhaps most importantly, always being my unconditional advocate in any way they could. Though some would consider having a thesis advisor change universities during their time in the lab to be a uniformly difficult occurrence, it gave me the amazing opportunity to have Dr. Ahn as a co-mentor, for which I feel incredibly fortunate. Thank you both, I will be forever grateful for the time and care you spent training me.

I would also like to thank my thesis committee: Drs. Sarah Millar, Maurizio Pacifici, Struan Grant, and Faye Mourkioti. Thank you for taking your time and effort to provide me helpful feedback and insight on my data over the last few years. My committee has been ever-supportive and accommodating throughout this dissertation.

Thank you to all of those I have worked with along the way, both here and in Michigan. Special thanks to: Dr. Jason Ashley, Dr. Peeyush Goel, Dr. Mike Dishowitz, John Hebb, Michele Lowe, Rob Zondervan, Katie Panos, Derek Dopkin, Jessica Applebaum, and Sarthak Mohanty. Thank you to those who helped me with my project from the McKay Laboratory and the Penn Center for Musculoskeletal Disease cores: Shereen Tamsen, Snehal Shetye, and Mac Sennett. And, of course, thank you to all my friends near and far that have supported me through the years.

I would also like to thank my parents for all their support and encouragement throughout my life. Thank you specifically for always encouraging me to learn and explore. To

iv

Jon, my love, thank you for supporting me day in and day out, always being up for an adventure, and just being you. It has been truly wonderful having you by my side during this thesis. And it's still a good dream, with cool animals in it.

And finally, to all my creatures (owned and fostered) – you make life worthwhile in ways I don't fully understand, and there is no way I could have made it through this endeavor without you. I hope we make as much of a difference in your lives as you do in ours.

ABSTRACT

R-SPONDIN-2 MODULATES OSTEOBLASTOGENESIS AND BONE ACCRUAL THROUGH

WNT SIGNALING

Meghan Noelle Knight

Jaimo Ahn

Kurt D. Hankenson

The R-spondin family of proteins are Wnt agonists, and the complete embryonic disruption of

Rspo2 results in skeletal developmental defects that recapitulate the phenotype observed with

Lrp5/6 deficiency. Previous work has shown that Rspo2 is both highly expressed in Wnt-

stimulated pre-osteoblasts and that its over-expression induces osteoblast differentiation in the

same cells, supporting its role as a positive autocrine regulator of osteoblastogenesis. However,

the role of Rspo2 in the autocrine regulation of osteoblastogenesis in postnatal bone is under

explored. Here, we show that limb-bud progenitor cells from Rspo2 knockout mice undergo

reduced mineralization during osteoblastogenesis in vitro, and have a corresponding alteration

in their osteogenic gene expression profile. The first Rspo2 conditional knockout (Rspo2^{floxed})

mouse was generated, and Rspo2 was knocked out in osteoblasts by crossing to the Osteocalcin-

Cre mouse line (Ocn-Cre+ Rspo2$^{f/f}$) to address the autocrine role of Rspo2 in vivo. Ocn-

Cre+Rspo2$^{f/f}$ male and female mice at 1, 3, and 6 months were examined. Ocn-Cre+Rspo2$^{f/f}$

mice are decreased in overall body size compared to their littermates, and they have decreased

trabecular bone mass due primarily to decreased trabecular thickness. Histomorphometric

analysis revealed a similar number of osteoblasts and mineralizing surface per bone surface with

a simultaneous decrease in mineral apposition and bone formation rates, suggesting that a

decreased mineralization capacity rather than an overall reduced number of osteoblasts is the

etiology of the reduced bone volume. In following with this, BM-MSC from Ocn-Cre+Rspo2$^{f/f}$

mice undergo less mineralization in vitro. Overall, Rspo2 loss reduces osteoblastogenesis and

mineralization both in vitro and in vivo, leading to reduced bone mass.

TABLE OF CONTENTS

ix

LIST OF TABLES

x

LIST OF FIGURES

CHAPTER 1: INTRODUCTION

A portion of this introduction and Figures 1.1 and 1.2 were published in a review in the journal Matrix Biology (Knight and Hankenson 2014)

1.1   Clinical Significance of Bone Mass Regulation

Bone possesses an incredible ability to repair and rebuild itself via continuous remodeling throughout an individual's life. This remodeling is not only necessary for repair, but is also essential to maintain the integrity of the skeleton. Imbalance of the remodeling process can lead to either too much or too little bone tissue, leading to conditions of low and high bone mass. For instance, osteoporosis is a condition characterized by low bone mass, micro-architectural deterioration of bone tissue, and increased risk of fracture (Kanis, 1994; Kanis et al., 1994). It affects more than 200 million people worldwide, and the incidence is continually rising with the increasing life expectancies of populations across the globe. The prevalence of overall low bone mass is even greater. Fractures, particularly of the hip, resulting from osteoporosis are a major cause of morbidity, disability, and premature mortality in older individuals, creating a huge economic burden (Johnell and Kanis, 2006; Dhanwal et al., 2011). In the United States alone, the financial burden of the more than 2 million osteoporosis-related fractures per year is estimated at US $19 billion (Burge et al., 2007). Women account for a larger proportion of both individuals affected by osteoporosis and those with osteoporosis-related fractures, due to the increased incidence of bone loss associated with menopause. This increased bone loss results in approximately 30% of postmenopausal women in the United States and Europe developing clinical osteoporosis. At least 40% of these women will sustain one or more fragility fractures during the remainder of their lifetime (Kanis, 2002).

While osteoporosis and low bone mass occur commonly in individuals of advanced age secondary to menopause and age-related bone loss, they also occur in cases of disuse, in certain

genetic and metabolic conditions, and treatment with specific medications. Disuse most commonly results from prolonged bed rest, spinal cord injuries and strokes that lead to paresis and paralysis, and immobilization due to an injury, such as casting. Less commonly, but no less importantly, low bone mass occurs rapidly in low-gravity environments (Bloomfield, 2010). Numerous genetic conditions lead to conditions of low bone mass, such as osteogenesis imperfecta and osteoporosis pseudoglioma syndrome (Karasik et al., 2016). Metabolic disruptions such as hyperadrenocorticism and hyperthyroidism, can also result in loss of bone mass (Fitzpatrick, 2002; Tuchendler and Bolanowski, 2014). Similarly, medications such as corticosteroids and heparin are also associated with reduced bone mass with long term use (Panday et al., 2014). Overall, there are many clinical conditions that lead to bone loss.

Conversely, dysregulation of bone remodeling can also lead to high bone mass. This is seen in several rare genetic conditions such as Sclerostosis, Van Buchem disease, and with Lrp5/6 gain-of-function mutations (Brunkow et al., 2001; Balemans et al., 2002; Boyden et al., 2002). These conditions can be clinically significant, with progressive bone growth leading to impingement of the cranial nerves due to stenotic foramina of the skull and subsequent auditory loss, visual loss, anosmia, increased intracranial pressure, and facial palsies. Malformations including syndactyly and mandibular hypertrophy are common in the more severe condition of Sclerostosis. Though there are only a few recognized clinical conditions of high bone mass to date, many mutations can lead to subclinical increases in bone mass, with reported resistance to fracture in high impact trauma and anecdotal reports of decreased buoyancy in water (Gregson et al., 2012). GWAS studies have further identified many loci that contribute negatively or positively to overall bone mass in both monogenetic and polygenetic manners, suggesting that there is still much to be investigated regarding normal variations and

2

subclinical changes in bone mass and how this relates to the clinical burden of fractures and osteoporosis (Karasik et al., 2016). Moreover, much like the reciprocal case for decreased bone mass, several metabolic conditions and medications, such as hypothyroidism and lithium chloride, can cause increases in bone mass.

The current therapeutics designed for osteoporosis treatment and prevention are limited in their scope and clinical effectiveness. The most commonly prescribed agents are the anti-resorptive bisphosphonates. While these are effective at preventing resorption, they do not promote increased bone production to further restore bone already lost. Denosumab is an antibody-mediated therapeutic targeted at RANK-Ligand (RANKL), that also functions through inhibition of bone resorption (Cummings et al., 2009). Teriparatide is a recombinant peptide drug based on parathyroid hormone and was the first anabolic agent approved to treat osteoporosis. Currently it is only labeled for those at high risk of fracture, and the length of treatment is limited (Bodenner et al., 2007). An agent related to teriparatide, abaloparatide, also was recently approved by the FDA (Radius Health, 2017). A second osteoanabolic therapeutic, romosozumab, is on track for approval this year (Lim and Bolster, 2017). This is an antibody targeting Sclerostin, an antagonist of canonical Wnt signaling in bone, and has been successful in clinical trials thus far. While these therapeutics do increase bone mass, there are significant limitations in treatment options and in clinical effectiveness, particularly in the realm of osteoanabolics.

It is clear that conditions of both low and high bone mass can be of considerable clinical significance. As will be discussed in the next section, the regulation of bone strength through bone mass and architecture is multifactorial and stems from a myriad of mechanisms. As a result, many conditions cause alterations in bone mass. Among these, osteoporosis is of

particularly considerable concern due to its extensive associated global morbidity, mortality, and economic burden, necessitating the discovery of novel therapeutics.

1.2   Bone Mass Regulation

Bone mass refers to the physical mass of bone tissue in the skeleton, with contributions from both the bone tissue volume as well as the density of the tissue. Together with bone architecture, it is the main determinant of the strength of the skeleton. In adults, bone mass is regulated through the precise balance and coupling of osteoclastic bone resorption and osteoblastic bone formation in a process known as bone remodeling. The primary functions underlying this process are the replacement of old or damaged bone, response to changes in mechanical stress, and calcium homeostasis (Harada and Rodan, 2003).

Remodeling occurs continuously throughout an individual's lifetime in response to numerous hormonal and mechanical signals, allowing the body to adapt to both metabolic and physical stresses. Bone remodeling begins with recruitment of bone-resorbing osteoclasts to the bone surface, followed by bone resorption. A reversal phase then occurs with the apoptosis of the osteoclasts and recruitment of bone-building osteoblasts. Finally, bone matrix deposition by the recruited osteoblasts replaces the resorbed bone (Figure 1.1). It is estimated that in healthy individuals, the adult skeleton is renewed entirely by this remodeling process every ten years (Manolagas, 2000).

There are many factors that can lead to an imbalance in the bone remodeling process, which in turn leads to overall loss or gain of bone mass. Systemic requirements for calcium are mediated primarily through parathyroid hormone (PTH) and can indirectly increase osteoclast activity and subsequent calcium release, whereas high serum calcium levels can stimulate the

4

release of calcitonin, which directly inhibits osteoclast activity to reduce further calcium release (Zuo et al., 2012). PTH also induces the activation of Vitamin D, which then stimulates osteoclast differentiation and decreases osteoblastogenesis (Bell et al., 2010). Mechanical loading and unloading both have strong and opposing effects on bone remodeling, which are mediated by numerous cellular signals (Bloomfield, 2010). Sex steroids have a significant impact on bone remodeling, as can be seen with the changes in remodeling following menopause, resulting from decreased estrogen levels. Estrogen does this primarily by decreasing the absolute osteoclast number, while testosterone can either increase bone mass indirectly by conversion to estrogen or through a direct effect on bone formation (Manolagas, 2000).

Beyond these metabolic influences on bone mass regulation, genetics are also incredibly important. Many polymorphisms and specific gene mutations have been associated with alterations in bone mass. GWAS analysis has revealed that many of these associated genes are i) part of the Wnt signaling pathway (e.g. LRP5/6, SOST, WNT3, WNT16, WTS, AXIN1, CTNNB1), ii) part of the hormonal signaling pathways mentioned above (e.g. Vitamin D Receptor, Estrogen Receptor, PTH), iii) involved in osteoblast differentiation and function (e.g. RUNX2, SP7, SMOC1), or iv) involved in osteoclast differentiation (e.g. TNFSF11, TNFRSF11A/B, CLCN7) (Karasik et al., 2016). Many of these genes have also been correlated with rare mutations that cause pathologic conditions of low bone mass. These GWAS findings corroborate and shed light on both already known and potential novel cellular and signaling mechanisms of bone mass regulation.

1.3   Osteoblastogenesis

Osteoblasts are critical to building and maintaining bone mass, and are responsible for the deposition of immature bone matrix, termed osteoid, on bone surfaces. Mesenchymal progenitor cells, sometimes referred to as mesenchymal stem cells (MSC), differentiate to

5

osteochondral progenitors, then subsequently undergo the differentiation to pre-osteoblasts, osteoblasts, and ultimately osteocytes. Critical regulatory points during this process include the renewal of MSC, the stimulation of precursor replication, the initiation of and progression through osteoblastogenesis, and the inhibition of osteoblast and osteocyte apoptosis. Since MSC can also differentiate into chondrocytes and adipocytes, another point of regulation is the inhibition of other differentiation towards these fates (Zuo et al., 2012).

The master regulator of osteogenesis is the transcription factor Runx2, and its expression is critical for the commitment of MSC to the osteoblast lineage. Osterix (Osx) expression increases following Runx2 expression, after mesenchymal condensation has occurred, and is a hallmark of the pre-osteoblast stages. Alkaline phosphatase (ALP), a protein essential for mineral metabolism in bone, is also expressed at this stage. After this, osteocalcin (Ocn), Type-1 Collagen (Col1), and bone sialoprotein (BSP) are expressed, marking the transition from pre-osteoblasts to immature osteoblasts (Bruderer et al., 2014). Osteocyte markers, such as Phex and Dmp1, are expressed as the osteoblasts mature into osteocytes in the bone matrix (Bonewald, 2011). Many cellular signaling pathways have identified roles in osteoblastogenesis, with Runx2 being a main point of integration for these signals. The canonical Wnt, BMP, and Notch signaling pathways have all been implicated as positive regulators, among others (Lin and Hankenson, 2011; Knight and Hankenson, 2013). Though this general sequence has been determined, and osteoblastogenesis can be monitored through these changes in gene expression, the precise control and transcriptional cascade involved in osteoblastogenesis and resultant effect on phenotype still need to be delineated.

6

1.4   The Wnt Signaling Pathway

Canonical Wnt signaling, functioning through beta-catenin stabilization, is involved in a wide array of physiologic developmental and homeostatic functions. As mentioned above, it is one of the primary signaling pathways involved in osteoblastogenesis and bone accrual, making it of critical importance to the study of osteoporosis and bone remodeling. There are also numerous noncanonical, or beta-catenin-independent signaling pathways with less established roles in bone (Monroe et al., 2012).

The canonical Wnt signaling pathway is activated when a Wnt ligand binds to its co-receptors at the cell surface. The core receptors in canonical Wnt signaling are the Frizzled family of G-protein-coupled receptors and the low-density lipoprotein receptor-related proteins 5 and 6 (LRP5 and LRP6). This ligand binding results in the recruitment of members of the beta-catenin destruction complex to the cell membrane. The beta-catenin destruction complex contains the proteins Disheveled (Dvl), Axin2, Glycogen synthase kinase 3beta (GSK3beta), Casein kinase 1 alpha (CK1alpha), and Adenomatosis polyposis coli (APC). In the absence of bound Wnt ligand, this complex recruits and phosphorylates beta-catenin, targeting it for ubiquitination and subsequent destruction in the proteasome. The complex is inactivated when members of this complex are recruited away from this complex following Wnt ligand binding, and stable, non-phosphorylated cytoplasmic beta-catenin accumulates. This beta-catenin can then translocate to the nucleus and interact with the Tcf/Lef family of transcription factors to alter gene transcription. Many extracellular modulators of Wnt signaling have been discovered, including the dickopfs (DKK), secreted Frizzled-related proteins (sFRP), Wnt Inhibitory Factor (WIF), and Sclerostin (SOST) (Nusse and Clevers, 2017).

7

In contrast to the beta-catenin signaling described above, noncanonical Wnt signaling does not stabilize beta-catenin. There are multiple noncanonical Wnt pathways that have been investigated, including the Wnt/Planar Cell Polarity Pathway (PCP) and Wnt/Ca^{2+} Pathway. In bone, the noncanonical pathway with the most evidence supporting a function role is the Wnt/PCP pathway (Caverzasio, 2009). Similar to canonical signaling, activation of this pathway is initiated by ligand binding to Frizzled and a co-receptor. However, co-receptors other than Lrp5/Lrp6 are utilized, and downstream signaling involves the small GTPases Rho, Rac, and JNK. In Wnt/Ca^{2+} signaling, calcium is released from the endoplasmic reticulum in response to Wnt ligand binding. This is thought to be mediated by the Frizzled receptors' G-protein coupling. Despite the often-described clear distinction between these canonical and non-canonical pathways, they are most likely integrated at various points along the signaling pathway. In fact, many of the various Wnt ligands have been shown to activate multiple Wnt signaling pathways depending on the context (Kobayashi et al., 2015; Kobayashi et al., 2016).

1.5   Wnt Signaling and Bone Mass Regulation

Canonical Wnt signaling is involved in regulation of the mature skeleton. Canonical signaling was first implicated in bone mass regulation in 2001, when mutations in the Wnt co-receptor LRP5 were found to be associated with a low bone mass phenotype in humans (Gong et al., 2001). Corresponding gain-of-function mutations in LRP5 resulting in a high bone mass phenotype were identified soon after (Boyden et al., 2002; Little et al., 2002). Mutations in the related Wnt co-receptor LRP6 lead to similar phenotypes. Polymorphisms in both receptors have also been correlated with bone mass. The role of canonical Wnt signaling in bone is further supported by loss-of-function mutations in sclerostin, a Wnt antagonist in bone, that lead to Sclerosteosis and Van Buchem Disease in humans. Furthermore, there is increased bone mass

8

seen with anti-sclerostin antibody administration in animal models and humans (Ominsky et al., 2010; Padhi et al., 2011; McClung et al., 2014).

Many murine models involving alterations of Wnt signaling have corroborated the positive role of canonical Wnt signaling on bone mass. Conditional knockouts of beta-catenin (Cttnb1) cause severe decreases in bone mass, with earlier disruptions also leading to skeletogenesis defects (Glass et al., 2005; Hill et al., 2005; Hu et al., 2005). Conditional deletions specifically in osteoblasts result in decreases in trabecular and cortical bone mass without skeletogenesis defects (Holmen et al., 2005; Kramer et al., 2010). Similarly, knockouts of Lrp5 and Lrp6 lead to decreased bone mass, even with limited disruption by knock out only in the osteocytes via Dmp1-Cre (Kato et al., 2002; Fujino et al., 2003; Holmen et al., 2004; Cui et al., 2011). Lrp6 homozygous knockout mice are perinatal lethal and have limb malformations resulting in missing digits (Pinson et al., 2000). When the Lrp5 and Lrp6 knockout models are bred together to create double knockouts, skeletogenesis defects occur with loss or reduction of digits. The most severely affected animals had complete loss of limbs, synostoses of carpal and tarsal bones, and only a single hindlimb digit (Holmen et al., 2004). Knockouts of Wnt3a or Wnt5a lead to reduced bone mineral density and trabecular number (Takada et al., 2007). Knockout of Wnt10b leads to progressive osteopenia, with decreased bone mineral density and trabecular number but no decrease in trabecular thickness (Bennett et al., 2005; Bennett et al., 2007; Stevens et al., 2010). Knockout of sclerostin and DKK, negative regulators of Wnt signaling, result in increased bone mass (Balemans et al., 2002; Morvan et al., 2006; Krause et al., 2010). While the phenotypes differ in severity, a general trend of decreased bone mass is observed among all disruptions of canonical Wnt signaling in bone.

9

1.6   Wnt Signaling and Osteoblastogenesis

Canonical Wnt signaling is involved in the induction of myogenic and osteogenic differentiation, as well as the inhibition of chondrogenesis and adipogenesis, making it a critical regulator of MSC lineage commitment (Day et al., 2005; Hill et al., 2005; Hu et al., 2005; Kennell and MacDougald, 2005). The stabilization of beta-catenin through canonical Wnt signaling has been found to have significant effects throughout osteoblastogenesis. In MSC, beta-catenin stabilization enhances commitment to and differentiation of the osteoblast cell lineage, with concomitant repression of differentiation along the chondrogenic and adipogenic lineages (Day et al., 2005; Hill et al., 2005; Hu et al., 2005; Kennell and MacDougald, 2005; Bennett et al., 2007; Miclea et al., 2009). Furthermore, proliferation and survival of osteoblasts is modulated by canonical Wnt signaling (Monroe et al., 2012). Osteoblasts and osteocytes also modulate osteoblast-osteoclast coupling in response to stabilized beta-catenin by producing osteoprotegerin, which inhibits osteoclasts (Glass et al., 2005). The data concerning the effects of Wnt signaling on osteoblasts have been corroborated by a large array of mouse models, demonstrating increased bone mass with increased beta-catenin stabilization in osteoblastic lineage cells, and reduced bone mass with decreased canonical signaling (Holmen et al., 2004; Hill et al., 2005; Holmen et al., 2005; Kugimiya et al., 2007; Cui et al., 2011; Wei et al., 2011).

1.7   R-spondins

The R-spondins, a family of four secreted proteins in the thrombospondin type 1 repeat (TSR1)-containing protein superfamily, are well recognized Wnt signaling agonists. Homologues of R-spondins are present in all vertebrates as well as select invertebrates, such as hemichordates, chordates, and echinoderms, but not *Drosophila* and *Caenorhabditis elegans* (Cruciat and Niehrs, 2013). In mammals, R-spondins have ~ 60% sequence homology,

10

and all R-spondins have a similar modular domain structure: an N-terminal putative signal sequence for secretion, two sequential cysteine-rich furin-like domains, a single TSR1, and a positively charged C-terminus (Hankenson et al., 2010; de Lau et al., 2012) (Fig. 1). The TSR1 domain contains conserved tryptophans and a conserved cysteine-rich CSVTCG domain, with the valine and threonine residues variably replaced with amine-containing side-group residues in different TSR1-domain-containing proteins. Specifically, each R-spondin has the VT residues replaced with two basic amino acids (either lysine or arginine), one or two polar amino acids (e.g. glutamine, asparagine) or in the case of Rspo3 and Rspo4, a single glycine.

Though Rspo3 was originally identified in 1971, as 'thrombin-sensitive protein' (Baenziger et al., 1971), the R-spondin family only began to be elucidated in 2002, with the discovery of Rspo1 (Chen et al., 2002) and subsequent discovery and characterization of the remaining members (Kamata et al., 2004; Kazanskaya et al., 2004; Kim et al., 2006). R-spondins are likely bound to heparan-sulfated proteoglycans in the extracellular matrix (ECM), as evidenced by their near lack of detection in the medium of transfected cells, their subsequent release with added soluble heparin, and their binding to Syndecan 4 (Nam et al., 2006; Ohkawara et al., 2011). However, potential interactions with other ECM molecules are not well-described.

The four R-spondin family members can potently activate canonical Wnt signaling in a Wnt-dependent manner, and their furin-like domains are necessary and sufficient for this activity (Kazanskaya et al., 2004; Nam et al., 2006; Kim et al., 2008; Glinka et al., 2011). The mechanism, and more specifically the receptor, for this activation has been highly debated for several years, with reports of Frizzled 8, low-density lipoprotein receptor-related protein 6 (LRP6), and Kremen all binding to R-spondins. However, none of these studies have been confirmed (Nam et al., 2006; Binnerts et al., 2007; Wei et al., 2007; Glinka et al., 2011;

11

Ohkawara et al., 2011). In 2013, the furin domain of the R-spondins was found to bind to leucine-rich repeat-containing G-protein-coupled receptors 4-6 (LGR4-6) (Chen et al., 2013) after several studies identified these as receptors for the R-spondins with a K_d in the nanomolar range (Carmon et al., 2011; de Lau et al., 2011; Glinka et al., 2011; Ruffner et al., 2012). The current proposed mechanism for the R-spondin-mediated activation of canonical Wnt signaling is the formation of a ternary complex of LGR, R-spondin, and the transmembrane RING-type E3 ubiquitin ligase ZNRF3 or RNF43 (Hao et al., 2012; Koo et al., 2012), which thereby alleviates ZNRF3/RNF43 membrane clearance of the Frizzled–LRP Wnt coreceptor complex (Hao et al., 2012) (Fig. 2). R-spondins can also enhance non-canonical Wnt/PCP signaling through the TSR1 domain during Xenopus development (Ohkawara et al., 2011). The ability of R-spondins to bind to structural extracellular matrix proteins, such as heparan-sulfated proteoglycans, along with their ability to bind cell surface receptors and potentiate Wnt signaling, clearly defines R-spondins as matricellular proteins.

R-spondin family member functions

<u>Rspo1</u>

The most prominent phenotype related to R-spondin 1 dysfunction is due to its role in gonadal development, with mutation leading to a rare form of XX male sex reversal (Parma et al., 2006). Rspo1 is expressed in the developing ovary, neural tube, kidney, stomach, dermis, mammary glands, limb bud, long bones, craniofacial bones, and vertebrae in the mouse (Nam et al., 2007b; Tomizuka et al., 2008). Rspo1-null mice have decreased fertility and lack duct branching and alveolar formation in the mammary glands, leading to a failure of lactation (Chadi et al., 2009). Systemic administration of Rspo1 in mice leads to a dramatic enlargement of the gastrointestinal tract with extensive proliferation of the crypt epithelial cells (Kim et al., 2005).

12

Rspo2

The major phenotypes associated with the global loss of R-spondin 2 during development are limb and craniofacial malformations and hypomorphic lungs due to defective branching, which result in perinatal death (Bell et al., 2008; Yamada et al., 2009). Rspo2-null mice also exhibit laryngeal–tracheal and kidney malformation. During development, Rspo2 is prominently expressed in the apical ectodermal ridge (AER) of the limb bud, and additional expression has been seen in the developing lungs, brain, pharynx, teeth, long bones, craniofacial bones, and vertebrae (Nam et al., 2007b). Rspo2 morpholinos injected into Xenopus embryos inhibited the expression of myogenic markers, suggesting a role for Rspo2 in myogenesis (Kazanskaya et al., 2004). Additionally, a 3'UTR insertion in the Rspo2 gene in dogs that increases the mRNA stability causes increased hair growth on the face and legs (Cadieu et al., 2009; Parker et al., 2010). Loss of Rspo2 reduces Wnt signaling activity in the area of expression, and genetic epistasis was observed when the skeletal phenotype of Rspo2 null mice was exacerbated by crossing to an Lrp6 knockout line, suggesting that the main mechanism of Rspo2 function is through the canonical Wnt pathway (Bell et al., 2008).

Rspo3

R-spondin 3 deficiency during development leads to vascular defects in the placenta of mice, with no penetration of fetal blood vessels into the chorion due to a lack of induction of VEGF expression in the placenta (Aoki et al., 2007; Kazanskaya et al., 2008). Rspo3 is highly expressed in the primitive streak during very early development and is also expressed in the developing neural tube, brain, limb bud, heart, kidney, and small intestine. However, embryonic death around embryonic day 10 (E10) limits the detection of further effects of Rspo3 deficiency (Nam et al., 2007b). Kazanskaya et al. describe a shift from blood cell specification to angioblast

13

specification with the addition of Rspo3 in vitro (Kazanskaya et al., 2008). Rspo3 is thought to be partially redundant with Rspo2 in hindlimb development due to observed increases in severity of defects in double mutant mice despite no observed effects of Rspo3 knockout alone in the limb bud mesenchyme (Neufeld et al., 2012).

<u>Rspo4</u>

The prominent feature of R-spondin 4 loss is anonychia, the absence of nails. Rspo4 is only weakly expressed in the developing neural tube, but there is much higher expression in the developing heart and limb buds (Bergmann et al., 2006; Nam et al., 2007b). Expression in the claw primordia in the mouse can also be detected (Bergmann et al., 2006). Mutations in Rspo4 that led to isolated anonychia are clustered in the two cysteine-rich furin-like domains, which are known to be important in the potentiation of canonical Wnt signaling by R-spondins (Brüchle et al., 2008).

1.8 R-spondins and Bone

R-spondins have recently been recognized as modulators of the skeleton. During development, all four R-spondins are expressed in the developing limb bud. Rspo1 has weak expression in the ectoderm and mesoderm at the junction of the limb bud and the trunk at embryonic stage 10.5 (E10.5). Much stronger expression is seen in the mesenchyme of the developing phalanges between E12.5 and E14.5. Robust Rspo2 expression in the limb bud is associated with the AER between E10.5 and E14.5 (Bell et al., 2003; Nam et al., 2007a). Rspo2 knockout mice are the only Rspo knockouts with a described skeletal phenotype, with loss of the autopod and fibula on the hindlimbs, loss of digits and some radii on the forelimbs, and the complete absence of nails coincident with the loss of the distal phalanx on all formed digits.

14

Cleft palates and craniofacial malformations have also been noted. This phenotype is consistent with a reduction in Wnt signaling as demonstrated in a variety of mouse models of disrupted Wnt signaling (Gong et al., 2001). Interestingly, this phenotype is more severe in the left hindlimb and the right forelimb (Bell et al., 2003). Double Rspo2/Rspo3 null mice have a more severe phenotype, suggesting at least partial redundancy despite a lack of skeletal phenotype in Rspo3 null mice alone (Neufeld et al., 2012). Rspo3 is expressed in the mesenchymal cells of the limb bud (between the expression of Rspo2 and Rspo4) at E10.5 and extends into the interdigitary spaces and nail primordia at E12.5 and E14.5, respectively. Rspo4 is expressed in the zone of polarizing activity, the anterior limb bud, and the most distal tips of the digits. These data suggest that Rspo2 and Rspo3 play a significant role in the maintenance of the AER and thus elongation of the limb bud and formation of distal structures. All R-spondins appear to play a role in the development of the most distal phalanges and nails. Additionally, all four R-spondins have some expression in the craniofacial bones and Rspo2 deletion results in malformation, suggesting a role for R-spondins in the development of these intramembranous bones (Nam et al., 2007a; Hankenson et al., 2010).

Current research supports a role for R-spondins in the mature skeleton, though studies are limited. Rspo1 synergizes with Wnt3A in C2C12 cells and primary murine calvarial cells in vitro, leading to increased osteoblastic differentiation (as measured by ALP activity and osteocalcin expression) and osteoprotegerin expression (Lu et al., 2008). Similarly, Rspo2 overexpression enhances MC3T3E1 osteoblastic differentiation (as measured by ALP activity, mineral staining, and gene expression) in the presence of BMP, and Rspo2 knockdown abrogates the enhanced differentiation seen with Wnt11 overexpression (Friedman et al., 2009). Rspo1 transcript levels increase in human primary osteoblasts and FOB1.19 cells during differentiation, and

15

recombinant Rspo1 administration can increase both beta-catenin stabilization and ALP activity in vitro (Sharma et al., 2013). Rspo1 levels also increased in response to vibration in vitro, and systemic administration of recombinant Rspo1 increased both mineral apposition rate and bone volume in three mouse models of aging known to have osteoporotic phenotypes (Wang et al., 2013). Deletion of the R-spondin receptor LGR4 in mice results in reduced bone mass due to both decreased bone formation and increased bone resorption, suggesting a role for R-spondins in mature bone maintenance (Luo et al., 2009). From a therapeutic perspective, recombinant Rspo1 injected into the joints of a murine arthritis model (TNFα overexpression — TNFtg) inhibited osteoclast development while stimulating osteoblast development, thus decreasing bone erosion and increasing cartilage integrity (Krönke et al., 2010). Furthermore, Rspo2 mRNA and protein expression is decreased in osteoarthritis (OA) patients. Rspo2 siRNA decreased mineralization of osteoblasts from healthy patients, and recombinant Rspo2 was able to increase the mineralization of osteoblasts from patients with osteoarthritis. Beta-catenin stabilization is also decreased in cells derived from OA patients, and recombinant Rspo2 is able to restore this stabilization to physiologic levels (Abed et al., 2011). Though many studies remain to be done, the R-spondin family provides a promising target for osteoanabolic therapeutics.

R-spondins are characterized as matricellular proteins on the basis of their expression in a variety of mesenchymal derived tissues, particularly the skeleton, and their ability to interact with both the extracellular matrix and a variety of cellular receptors. In the skeleton, R-spondins clearly have pro-osteoblastic effects; additionally, Rspo2 and perhaps Rspo3 regulate the process of endochondral ossification. R-spondins regulate Wnt/beta-catenin signaling, and the effects of R-spondins on osteoblasts and limb development are consistent with a reduction in beta-catenin stabilization and subsequent signaling. A number of questions remain concerning

16

the role of R-spondins in the skeleton, including the functional redundancy of the family

members, demonstrating the signaling mechanisms of R-spondins in skeletal cells, and

understanding the regulation of R-spondin expression and activity during skeletogenesis, the

maintenance of adult bone mass, and bone healing.
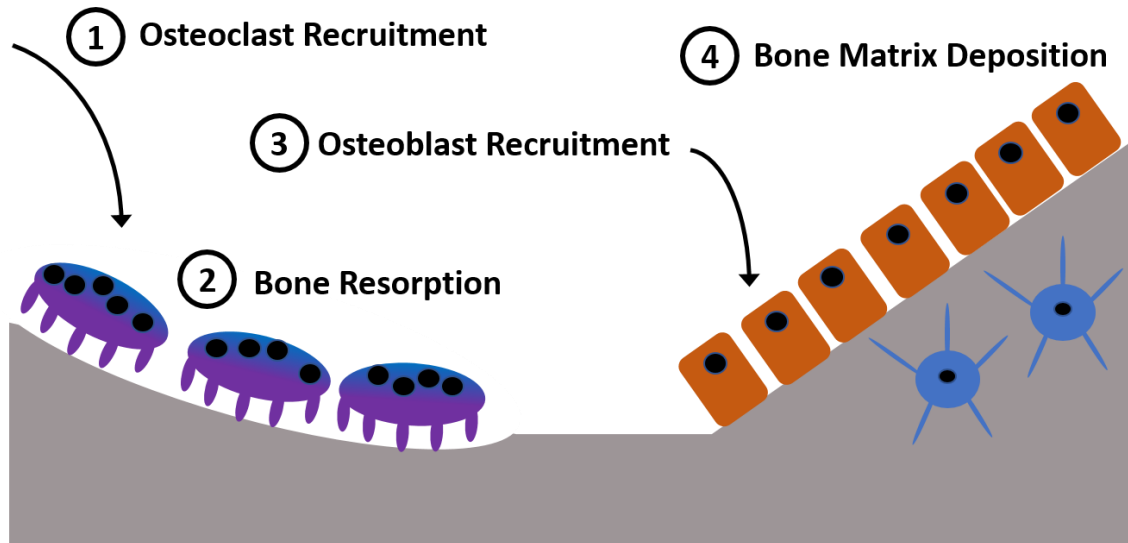
Figure 1.1. Bone remodeling. 1. Bone remodeling begins with the activation and recruitment of bone-resorbing osteoclasts (purple) to the bone surface. 2. This is followed by osteoclastic bone resorption. 3. A reversal phase then occurs with the apoptosis of the osteoclasts and recruitment of bone-building osteoblasts (orange). 4. Finally, bone matrix deposition by the recruited osteoblasts replaces the resorbed bone. Osteocytes (blue) are terminally differentiated osteoblasts that have become surrounded by the newly formed bone matrix during remodeling.
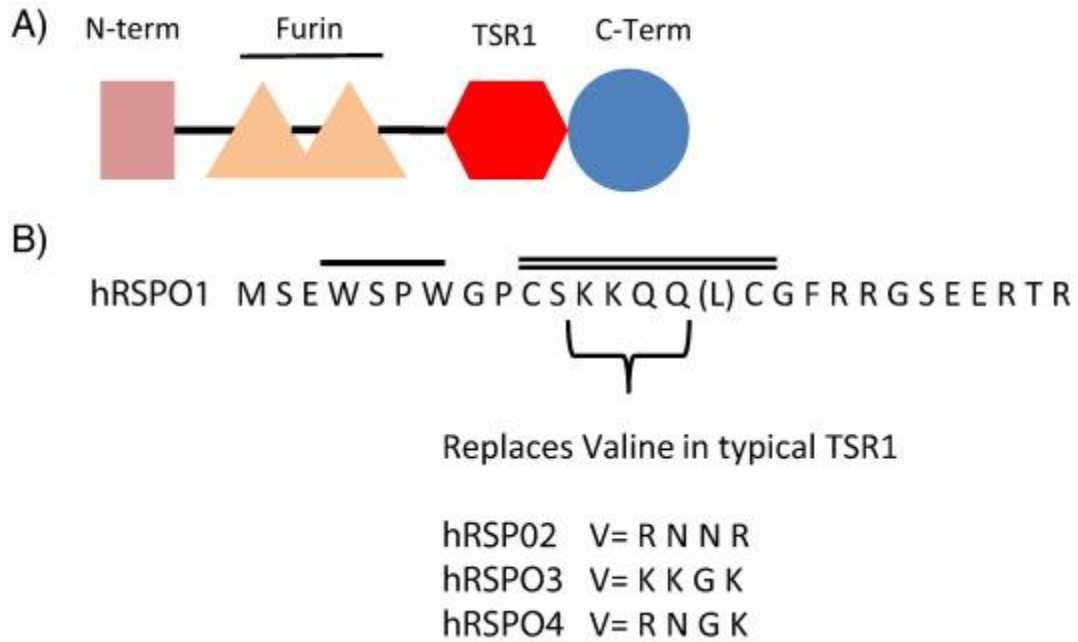
Figure 1.2. Structure of R-spondin. (A) R-spondins contain an N-terminus that contains a putative secretion signal, two furin repeats in a furin domain, a TSR1 domain, and a C-terminus. (B) The TSR1 domain of R-spondin conserves both the tryptophan rich region (single line) and the cysteine-rich CSVTCG region (double line). The valine in the prototypical TSR1 is replaced in the R-spondins with four amino acids that are basic and polar.
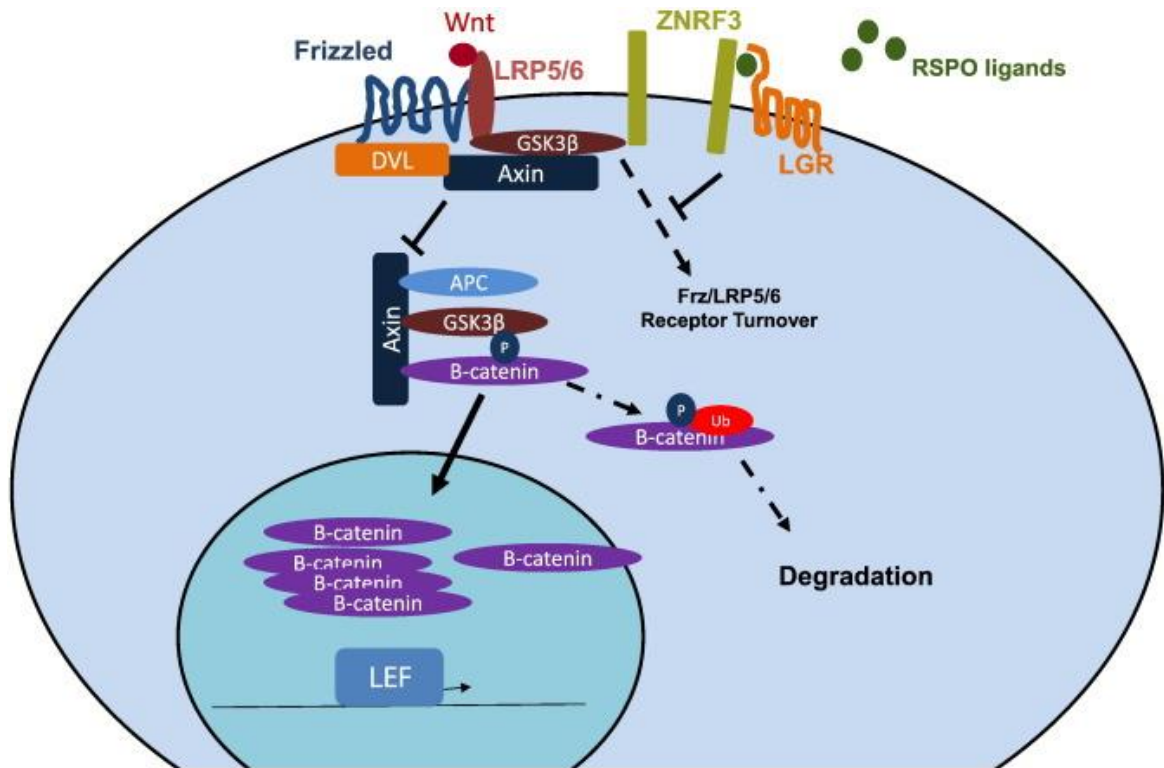
Figure 1.3. Signaling by R-spondin. This diagram demonstrates the role of R-spondin in regulating canonical Wnt signaling. During the process of canonical Wnt signaling, Wnt binds to Frizzled and LRP5/6. This binding promotes interaction with Axin. When Axin is bound to the receptor complex, this prevents Axin interaction with GSK3beta and APC. GSK3beta is then unable to phosphorylate beta-catenin which results in beta catenin stabilization and nuclear localization to interact with TCF/LEF transcription factors. When GSK3beta is active it results in beta-catenin phosphorylation and increased beta-catenin degradation following ubiquitination and proteasomal degradation. R-spondins regulate this canonical signaling process by inhibiting the action of ZNRF3. ZNRF3 acts as a Wnt signaling inhibitor by promoting LRP/Fzd turnover. When Rspo is bound to a LGR receptor it blocks the turnover inhibiting activity of ZNRF3.

CHAPTER 2: R-Spondin-2 is an osteoblast-produced Wnt agonist that regulates osteoblastogenesis

2.1 INTRODUCTION

Bone remodeling is critical for the maintenance of bone mass and structure, and is particularly important when considering pathologies that disrupt homeostasis, such as those that lead to the development of low-bone mass and osteoporosis. This decrement in bone mass and structure and the concordant decrease in mechanical strength can be caused both by dysregulation of osteoblastic and osteoclastic activity (Langdahl et al., 2016). Therapeutics to restore bone mass and strength therefore focus on targeting one of these two processes.

A potent positive regulator of bone deposition by osteoblasts during bone modeling and remodeling is the canonical Wnt signaling pathway, making it a highly desirable target for therapeutics to increase bone formation. The Wnt pathway has been deeply investigated in the context of bone, focusing on both extracellular pathway modulators and the stabilization of beta-catenin and transcription factors, generally with increases in canonical signaling through the pathway leading to increased osteoblastogenesis and bone formation (Monroe et al., 2012). Modulation of the pathway through antibodies targeting Sclerostin, an antagonist of canonical Wnt signaling in bone, has been particularly successful (Lim and Bolster, 2017). These antibodies, along with PTH and PTHrP analogs teriparatide and abaloparatide, are currently the only osteoanabolic therapeutics; other interventions primarily focus on inhibiting the further resorption of bone by osteoclasts, such as the bisphosphonates (Fukumoto and Matsumoto, 2017). There remains a critical need for the identification of additional osteoanabolic therapeutic options given the limitations, in terms of clinical use of the currently available therapeutics.

21

The R-spondin proteins, a family of four secreted matricellular proteins, potentiate Wnt signaling and may represent a novel focus of therapeutic targeting to modulate osteoblasts. The R-spondins activate canonical Wnt signaling by binding to the Leucine-Rich Repeat-Containing G-Protein Coupled Receptors 4-6 (LGR4-6), which then interacts with the E3-Ubiquitin ligases ZNRF3/RNF43 to inhibit Wnt receptor turnover (Hao et al., 2012; Koo et al., 2012). R-spondins are also reported to activate non-canonical Wnt/Planar Cell Polarity (PCP) signaling (Ohkawara et al., 2011). All four R-spondin family members have a similar modular domain structure: an N-terminal signal sequence, two furin-like/cysteine-rich domains, a thrombospondin type-1 motif (TSR1), and a basic amino acid rich C-terminus, which are encoded on separate exons (Hankenson et al., 2010). Each of the R-spondins are expressed in the developing mouse limb, as well as in other tissues, and each has different functional effects with respect to the skeleton. R-spondin-1 (Rspo1) disruption is not associated with a skeletal phenotype, but its expression is induced during osteoblastogenesis and in response to vibration (Wang et al., 2013). The Rspo2 knockout mouse (Rspo2^{ftl}) is perinatal lethal due to defective lung development and exhibits limb and craniofacial malformations (Bell et al., 2003; Bell et al., 2008). Our laboratory has previously demonstrated that Rspo2 is highly expressed in Wnt11-overexpressing pre-osteoblasts. Furthermore, both overexpression and recombinant addition of Rspo2 enhanced osteoblastogenesis in vitro (Friedman et al., 2009). Rspo3 disruption is embryonic lethal due to angiogenic defects in the murine placenta, though conditional knockout in limb mesenchyme (via Prx1-Cre recombinase-mediated disruption) exacerbated Rspo2 limb malformations in double knockouts (Aoki et al., 2007; Neufeld et al., 2012; Knight and Hankenson, 2014). Rspo4 mutations in humans lead to anonychia, but a skeletal phenotype has not been identified

22

(Bergmann et al., 2006; Nam et al., 2007b). It is clear that R-Spondins influence several aspects of skeletal biology, but their cell-specific roles in vivo have yet to be elucidated.

The clear anabolic in vitro effects of Rspo2 on osteoblastogenesis led us to investigate the mechanisms through which Rspo2 affects osteoblastogenesis. We utilized limb bud progenitor cells from the global knockout Rspo2[ftl] mouse model to evaluate Rspo2-deficient osteoblastogenesis in vitro. Further, due to the perinatal lethality of this model, we generated a conditional floxed Rspo2 allele. We crossed this model to a pan-expressing Cre mouse (EIIa-cre) and recapitulated the complete knockout phenotype. Next we crossed the floxed mouse to a mouse line that expresses Cre-recombinase under the control of the Osteocalcin (Ocn) promoter for specific recombination in osteoblasts to determine the function of Rspo2 in osteoblasts in postnatal bone. At 1 month, 3 months, and 6 months of age, we evaluated the skeletal phenotype of these mice by μCT, histomorphometry, mechanical testing, and analysis of progenitor cell populations. Herein, for the first time, we show that Rspo2 is an osteoblast autocrine factor that impacts bone development and adult bone mass accrual.

23

2.2 METHODS

Animals:

Animals were housed in a pathogen-free vivarium in accordance with institutional policies.

Rspo2^{ftl} mice were used for limb bud mesenchymal progenitor cell isolation. Ella-Cre mice were

obtained from Jackson Laboratories. Ocn-Cre mice were obtained from Dr. Tom Clemens, Johns

Hopkins University (Zhang et al., 2002). Mice were humanely euthanized at 1, 3, and 6 months

of age for skeletal phenotyping.

Generation of Rspo2^{flox} mice:

To create the Rspo2 conditional, or floxed, allele (Rspo2^{floxed}), we generated a targeting

construct in which a 2.9 kb genomic DNA fragment containing exons 4 and 5 was flanked by loxP

sites (Fig. 1a). The 5' homology arm was 2.9 kb in length and the 3' homology arm was 4.7 kb in

length. We used the targeting construct, which also contained a neomycin resistance cassette

flanked by Frt sites, to electroporate V6.5 ES cells, which are derived from C57BL/6 x 129/Sv

hybrid embryos. ES cell clones were identified as targeted by Southern blot analysis using

probes flanking the 5' and 3' ends of the targeting construct. ES cell lines were then karyotyped,

and one targeted line with no karyotype abnormalities was injected into C57BL/6 embryos to

generate chimeric mice. Subsequently, we crossed Rspo2^{flox} mice with C57BL/6 mice for 4 to 6

generations before crossing them with mice expressing the Cre recombinase.

Cell type-specific deletion of Rspo2^{fl} allele:

The Cre-transgenic mice used in this study have been previously described: EIIa-Cre (Lakso et al.,

1996) and Ocn-Cre (Zhang et al., 2002). We crossed hemizygous Cre transgenic mice with

homozygous Rspo2^{flox} mice to generate heterozygous Rspo2^{flox} offspring with and without a Cre

24

allele. We then crossed homozygous Rspo2^{flox} mice with heterozygous Rspo2^{flox} mice to generate

the following offspring: WT mice, mice hemizygous for a Cre allele, mice homozygous for the

Rspo2^{flox} allele, hereafter referred to as Rspo2$^{f/f}$, and Rspo2$^{f/f}$ mice that were also hemizygous for

a Cre allele. We genotyped offspring by PCR using the following primer sequences: Cre-for, 5'-

TTACATTGGTCCAGCCACC-3', Cre-rev, 5'-ACCAGCCAGCTATCAACTCG-3', product size 102 bp;

Rspo2-floxB-for, 5'-GCACTGTCCAGGAGGTAGGTCTAAAC-3', Rspo2-floxB-rev, 5'-

CCTTCTTCTGAGCACCATCTGC-3', product size 359 bp (WT) and 413 bp (floxed allele). Rspo2-

floxB-for and Rspo2-floxB-rev were combined with Rspo2-floxA-for 5'-

GACTCTTACTGCCTGGGATCCTCATT-3' to assess recombination with a product size of 512bp.

Skeletal Preparations:

Rspo2$^{f/f}$ males were time-mated with Rspo2$^{f/+}$;Ella-Cre+ females. e16.5 and e18.5 mouse

embryos were harvested, digested, and stained with Alizarin Red S and Alcian Blue by standard

methods (Rigueur and Lyons, 2014).

Micro-Computed Tomography:

Femurs were dissected, cleaned of soft tissue, and wrapped in PBS-soaked gauze. The wrapped

femurs were loaded into 9.0 mm diameter scanning tubes and imaged in a micro-computed

tomography (μCT) scanner (model μCT50, Scanco Medical, Wayne, PA, USA). Femurs were

scanned using the following parameters: 6.0 μm isotropic voxel size, 55kVp, 145 μA, 1000

projections per 180°, and 1500 ms integration time. Cortical bone parameters were measured

by analyzing 50 slices in the mid-diaphysis. This defined region was the central portion between

the proximal and distal ends of the femur. A semi-automated contouring method was used to

determine the outer cortical bone perimeter. Briefly, a user-defined contour was drawn around the cortical bone perimeter of the first slice. This initial estimate was then subjected to automated edge detection. This contour then served as the initial estimate for the next slice, with the contouring process continued for all 100 slices. A fixed, global threshold (300mg HA/cm^3) of the maximum gray value was used to distinguish bone from soft tissue and marrow. Trabecular bone parameters were measured by analyzing 150 slices of the distal metaphysis. Briefly, the distal end of the analysis region was chosen to be just proximal to the end of the primary spongiosa in the marrow cavity. This assured that only trabecular bone was analyzed. Starting at this image, a user-defined contour was drawn to include trabecular bone within the marrow cavity and exclude cortical bone. User-defined contours were drawn every 15-30 slices and an automated morphing program was used to interpolate the contours for all images in between. A fixed, global threshold of 220 mg HA/cm^3 was used to distinguish trabecular bone from soft tissue and marrow. A Gaussian low-pass filter ($\sigma = 0.8$, support = 1) was used for all analyses. Nomenclature is reported as previously described(Bouxsein et al., 2010).

Histology:

Tibias were dissected and fixed in fresh 4% paraformaldehyde at 4º C for 24 hours and then decalcified in 12% EDTA for 1 week. After decalcification, tibias were embedded in paraffin and 7um longitudinal sections were obtained. Hematoxylin and Eosin (H&E) and Alcian Blue Hematoxylin/Orange G (ABH/OG) staining was done by standard methods. For staining of tartrate-resistant acid phosphatase (TRAP), after de-paraffinization and rehydration, sections were incubated with acetate buffer containing naphthol-AS-BI-phosphate and Fast Red Violet at 37ºC for 30 minutes. The sections were then counterstained with 0.1% Fast Green.

Histomorphometry:

For dynamic histomorphometric analysis of bone formation, all animals were labeled with alizarin complexone and calcein. At 4, 6, or 8 days before euthanasia (for 1-, 3-, and 6-month-old mice, respectively), alizarin complexone was administered subcutaneously at a dose of 30mg/kg. At 1 day before euthanasia, calcein was administered subcutaneously at a dose of 20mg/kg. At harvest, right tibias were stripped of soft tissues, bisected, and immediately fixed in 70% ethanol under vacuum. Tibias were embedded in methyl methacrylate without decalcification. Sagittal sections of the proximal portion of the tibias were cut at 6μm thickness, and sections were stained with Goldner's Trichrome. Histomorphometrical analysis was performed using BioQuant® OSTEO Software. All parameters were calculated according to the recommendations of the Histomorphometry Nomenclature Committee of the American Society of Bone and Mineral Research (Dempster et al., 2013).

Biomechanical Testing:

Right femora were subjected to 3-point bending by standard techniques after microCT analysis at the Penn Center for Musculoskeletal Disorders Biomechanics Core. Femora were loaded in the anterior-posterior direction at 0.03 mm/s using a electromechanical testing machine (Instron 5542, Instron Inc., Norwood, MA) with the posterior side in tension between lower supports that were 7.66mm apart for the 1-month samples and 11.79mm apart for the 3-month and 6-month samples, with the upper loading pin in the center of the lower supports. All bones were tested at room temperature and kept moist with PBS. Crosshead displacement was obtained via the Instron system and load data were collected with a 10N load cell (Instron Inc., Norwood, MA) at a sampling frequency of 100 Hz. Load-displacement curves were analyzed for

27

whole bone stiffness and ultimate load using custom computational code (MATLAB R2015a; Mathworks Inc., Natick, MA, USA).

Bone Marrow-Derived Cell Culture:

Bone marrow cells were harvested from the left femur of 1-, 3-, and 6-month old mice. Whole marrow was expelled from the bone with several flushes through a 25-gauge needle. Single-cell suspensions were made by aspiration and expulsion of the marrow through an 18-gauge needle. Cells were strained through a 70μm cell strainer and then counted. Cells were pelleted and resuspended in MSC media (αMEM supplemented with 10% FBS, L-glutamine, 100IU/mL penicillin, 100mg/mL streptomycin). $4x10^6$ cells were plated on 60mm dishes in duplicate for CFU-F analysis. Colonies were allowed to grow for 12 days and then stained for Alkaline Phosphatase with Fast Red as a counterstain. Colonies were counted using a dissecting microscope. The remaining cells were plated on 100mm dishes for expansion. At the first passage, cells were seeded at $2.5 x 10^4$ cells/cm^2 into 48-well tissue culture plates and grown to confluence in MSC media, at which point they were cultured in osteopermissive media (OPM: αMEM supplemented with 10% fetal calf serum, 100x L-glutamine, 100 IU/mL penicillin, 100 mg/mL streptomycin, 32.3 μg/mL ascorbic acid 2-phosphate, 5 mM β-glycerophosphate). Cells were then fixed in formalin for 10 minutes and incubated in 2% Alizarin red S (pH 4.25) for 20 minutes. Excess Alizarin red S was removed and then calcium-bound Alizarin was extracted by treating with 10% (w/v) acetic acid, heating, and adjusting the pH to 4.1-4.5 with 10% ammonium hydroxide. Total mineral content was then measured colorimetrically at 405 nm using a spectrophotometer.

28

Limb Bud Mesenchymal Progenitor Cell (MPC) Culture:

Heterozygous Rspo2[ftl] mice were time-mated and embryos were harvested at e16.5. Limbs were dissected from the embryos, stripped of their autopods and soft tissues, and minced. They were then placed in media and aspirated and ejected through an 18-gauge needle 10 times. The media and tissue mixture was then plated on a 10cm plate and the adherent population was selected. The resultant cells are able to undergo osteogenesis as seen by ALP staining and Alizarin red S staining of mineral, as well as adipogenesis as seen by Oil Red O staining of lipid (data not shown). For osteogenesis, cells were seeded at 2.5×10^4 cells/cm^2 in 6- or 48-well tissue culture plates. The next day, cells were transferred to osteogenic media (OGM: αMEM supplemented with 10% fetal calf serum, 100x L-glutamine, 100 IU/mL penicillin, 100 mg/mL streptomycin, 32.3 μg/mL ascorbic acid 2-phosphate, 5 mM β-glycerophosphate, 2.5nM rhBMP-6 [R&D Systems]). 10nM Recombinant RSPO2 [R&D systems] was added during rescue experiments. Protein isolation was performed at 24 hours for western blotting. RNA isolation occurred at 24 hours, 5 days, 10 days, and 15 days. ALP staining occurred at 5 and 7 days. Alizarin red S staining of mineral occurred at 10 days, 15 days, and 20 days.

Western Blotting:

Cells were lysed in RIPA buffer in the presence of Phosphatase and Protease Inhibitor cocktails (Pierce and Roche, respectively). Lysates were separated on 4-20% gradient SDS-PAGE gels and transferred to nitrocellulose membranes. After blocking with Odyssey Blocking Buffer (Licor) for 30 min, blots were incubated with the following primary antibodies: Anti-RSPO2 (sc-292494, sc-74883), Anti-Active Beta-Catenin (Millipore 05-665), Anti-Total Beta-Catenin (BD Transduction

610154), and Anti-Beta-Tubulin (Sigma T7816). This was followed by incubation with the appropriate secondary antibody (Li-Cor) and imaging on a Li-Cor Odyssey CLx.

Gene Expression:

Cells were collected in TRIzol Reagent for RNA isolation. The Directzol RNA isolation kit (Zymo) was used for RNA purification according to the manufacturer's instructions. 1µg RNA was reverse-transcribed to cDNA using the Applied Biosystems High-Capacity cDNA Reverse Transcription kit. Gene expression was quantified using a ViiA 7 Real-Time PCR System (Applied Biosystems) with a 10µL reaction volume containing: 0.5µL cDNA, 0.5µM forward and reverse primers, and 1x PowerUp SYBR Green Master Mix (Applied Biosystems). For each gene of interest, samples were analyzed in triplicate and control wells were simultaneously analyzed to rule out DNA contamination and primer dimer binding. Proper amplicon production was confirmed by melt curve analysis. Data were normalized to the housekeeping gene 18S rRNA and presented as fold-change expression relative to WT whole bone, calculated using the formula $2^{-\Delta\Delta C(t)}$. 18S C(t) values were stable across treatment groups. Primer sequences are available upon request.

Statistics:

Two-way ANOVA or Student's t-test was used to detect statistically significant treatment effects, after determining that the data were normally distributed and exhibited equivalent variances. All t-tests were two-sided and unpaired. Tukey corrections were used for multiple comparisons during the two-way ANOVA. P-values less than 0.05 were considered statistically significant. While statistically significant differences do exist between male and female mice of both control

and Rspo2$^{f/f}$ mice, they are consistent with well-established sex differences in bone geometry in mice and are not reported herein.

2.3 RESULTS

Rspo2-null Limb-bud Mesenchymal Progenitor Cells have defective osteoblastogenesis

Our previous work demonstrated that Rspo2 was required for Wnt11-mediated osteoblastogenesis in MC3T3E1 cells, but the autocrine role of Rspo2 in primary osteoblasts was not examined (Friedman et al., 2009). MSC were harvested from Rspo2^{Ftl} mouse limb bud mesenchyme. These cells undergo osteoblast differentiation in the presence of BMP but not with ascorbic acid and inorganic phosphate alone. MSC isolated from Rspo2^{Ftl} mice (deficient in Rspo2) showed reduced osteoblastogenesis (Figure 2.1). Mineralization was significantly reduced in Rspo2^{Ftl} MSC compared to MSC from wildtype littermates (Figures 2.1A,B), a difference that could be rescued with the addition of recombinant RSPO2 to the media (Figure 2.1C). Despite the contrast in mineralization, there was no apparent difference in alkaline phosphatase staining between the genotypes (Figure 2.1D). To better understand the mechanism of reduced mineralization in the Rspo2 deficient cells, osteogenic gene expression was studied using RT-qPCR. There was no difference in the expression of Runx2, the master regulator of osteogenesis (Figure 2.1E). However, the downstream early marker of osteogenesis, Osterix (Osx), was significantly reduced in the Rspo2^{Ftl} MSC after 5 days of osteogenesis (Figure 2.1F) and remained decreased over the course of osteoblastogenesis (data not shown). The late-stage osteoblastogenesis marker of osteoblasts, Osteocalcin (Ocn), had reduced expression in the Rspo2^{Ftl} cells at 10 days of differentiation (Figure 2.1G), though this difference diminished with further differentiation (data not shown). In contrast, bone sialoprotein (BSP), another late-

31

stage osteoblastogenesis marker that is involved in the mineralization of the matrix, did not

show differences in expression in the Rspo2^{Ftl} MSC compared to the wild-type control cells

(Figure 2.1H).

Generation of R-Spondin-2 Conditional Allele

The perinatal lethality of the Rspo2 knockout mice prevents the examination of the impact of

Rspo2 on osteoblastogenesis and bone formation in post-natal bone. The R-spondin-2 allele

proved difficult to target using the most common strategies for loxP site selection as the gene

contains very large introns that are in-frame. Thus, we targeted the disruption of the Furin and

TSR repeats of the R-spondin-2 gene (Figure 2.2A). Previous work has shown that such

disruption results in a complete disruption of beta-catenin-mediated function (Kim et al., 2008).

A targeting construct with loxP sites flanking exons 4 and 5 was designed and used to target

V6.5 ES cells. ES Cells were screened for appropriate targeting by Southern blot analysis for both

arms of the construct, PCR identification of the downstream loxP site, and karyotype analysis.

Injection of the successfully targeted ES cells into C57BL/6 blastocysts resulted in 13 chimeric

pups, which were crossed to C57BL/6 mice for production of the F1 generation and

determination of germline transmission. Of the 43 F1 mice produced, 17 were confirmed via

PCR to be heterozygous for the targeted allele for both loxP sites. The construct was determined

to be intact via Southern blot analysis for both arms of the targeting construct. The targeting

construct was designed with an intronic deletion permitting the use of a single pair of PCR

primers flanking the downstream loxP site for genotyping. The floxed allele yields a 359bp

fragment, while the wild-type allele yields a 413bp fragment. The genotyping can also be

combined with the forward primer from the upstream loxP site for determination of

recombination when Cre recombinase is present, which yields a 512bp fragment (Figure 2.2B).

32

When this construct was expressed in cells with Cre-recombinase, an antibody corresponding to the C-terminus of RSPO2 confirmed decreased RSPO2 protein levels compared to cells not expressing Cre-recombinase (Figure 2.2C).

Recapitulation of Rspo2ftl Phenotype with Ella-Cre Expression

To test the functional significance of the Rspo2 allele in vivo, Rspo2^{floxed} mice were crossed with the pan-Cre expressing EIIa-cre mouse line, which has whole-body Cre-recombinase expression when the allele is inherited from the dam. Three litters from f/f Cre-negative x f/wt Cre-positive matings were aged to weaning. At P21, no EIIa-Cre+Rspo2$^{f/f}$ mice were identified. The genetic frequency was consistent with perinatal lethality of the EIIa-Cre+Rspo2$^{f/f}$ mice similar to the Rspo2^{Ftl} global knockout (Tables 1-2), with the other four possible genotypes each accounting for approximately one third of the total offspring. Skeletal preparations of E16.5 and E18.5 pups from similar matings were stained with Alcian blue and Alizarin red S. All Ella-Cre+Rspo2$^{f/f}$ pups had dysmorphic distal phalanges with decreased mineralization (10/10 embryos), and several pups additionally had reduced (8/10 embryos) or absent digits (4/10 embryos) (Figures 2.2D-I), consistent with the phenotype of the three models of Rspo2 global knockouts that have been previously published (Bell et al., 2003; Nam et al., 2007a; Aoki et al., 2008; Bell et al., 2008; Yamada et al., 2009). As may be expected with a Cre mediated knockout, there was heterogeneity in the embryo phenotypes. Figures 2.2E and 2.2H show the least severe phenotypes of the pelvic and thoracic limbs, respectively, with reduced distal phalangeal mineralization in the distal limb. Figures 2.2F and 2.2I show limbs of more severely affected individuals.

33

Osteoblast-specific knockout results in decreased body size, bone mass, and bone strength

Next, the Rspo2^{floxed} mice were crossed with Osteocalcin-Cre mice to disrupt Rspo2 selectively in mature osteoblasts.   Mice were measured (length and weight) at 3 weeks of age and then harvested at 1 month, 3-month, and 6-months of age for skeletal analysis of juvenile, young adult, and mature adult bone, respectively. At 3 weeks of age, targeted (homozygous Rspo2^{floxed}, Ocn-Cre-positive, herein referred to as Ocn-Cre+Rspo2$^{f/f}$) mice weighed less and had shorter crown-rump measurements than their control (homozygous Rspo2^{floxed}, Ocn-Cre-negative, herein referred to as WT) littermates (Figures 2.3A-C). At all timepoints, the femurs of Ocn-Cre+Rspo2$^{f/f}$ mice were significantly shorter than those of their control littermates (Figures 2.3D-F). Microcomputed Tomography (μCT) was used to evaluate trabecular and cortical bone of the right femur from mice at all timepoints. The phenotype was most pronounced at 3 months of age. At this timepoint, bone volume (BV) and bone volume fraction (BV/TV) were significantly decreased in the Ocn-Cre+Rspo2$^{f/f}$ mice, with trabecular thickness being the main contributor to this difference (Figures 2.4A-C). The difference in trabecular bone was more pronounced in male mice, with female targeted mice only trending to have decreased trabecular bone. Trabecular and cortical tissue mineral densities were not different between groups (Figures 2.4D,E). In cortical bone, 3-month-old mice had decreased cortical bone volume, decreased cortical thickness, decreased endosteal and periosteal perimeters, and decreased polar moment of inertia (Figures 2.4F-I). However, when males and females are considered separately, only targeted male mice showed significant reductions in these parameters. At 1 month of age, Ocn-Cre+Rspo2$^{f/f}$ mice had decreased BV and BV/TV compared to their control littermates (Figure 2.5A-B). The decreased BV/TV ratios corresponded to both decreased trabecular number and decreased trabecular thickness (Figures 2.5C-D). The tissue mineral density of the trabecular

34

bone and cortical bone did not differ across genotypes (Figure 2.5D-E). At 1 month of age, no significant differences were identified in the cortical bone parameters (Figures 2.5F-H). At 6 months of age, Ocn-Cre+Rspo2$^{f/f}$ mice demonstrated decreased BV and BV/TV, which was again primarily due to decreased trabecular thickness rather than trabecular number (Figures 2.6A-C). The tissue mineral densities of trabecular and cortical bone were not different between groups (Figures 2.6D-E). While cortical BV and cortical thickness still showed a decreasing trend in the Ocn-Cre+Rspo2$^{f/f}$ mice at 6 months, these parameters were no longer statistically significant (Figures 2.6F). Endosteal and periosteal perimeters and polar moment of inertia were not different between groups (Figure 2.6G-H, data not shown). Three dimensional reconstructions of trabecular and cortical bone of mice from the middle BV/TV and cortical thickness, respectively, are shown (Figures 2.4I-J, 2.5I-J, 2.6I-J). Right femora were subjected to biomechanical testing via 3-point bending. At 3 months of age, Ocn-Cre+Rspo2$^{f/f}$ mice had decreased maximum load force, corresponding to a weaker bone. They also had significantly decreased bending stiffness (Figures 2.4K-L). There were no differences in the maximum load force or bending stiffness at 1 month of age, however at 6 months of age, the male mice had decreases in both parameters (Figures 2.5K-L, 2.6K-L).

Osteoblast-specific Rspo2 knockout mice have decreased bone mass and mineral apposition rate
Static and dynamic histomorphometric analysis of trabecular bone of proximal tibiae from 1-month-old mice was performed to further assess bone microarchitecture as well as to assess bone formation. Representative histologic sections from WT (Figures 2.7A,C) and Ocn-Cre+Rspo2$^{f/f}$ (Figures 2.7B,D) littermate mice are shown. TRAP-stained sections and double-labeled bone sections from WT (E,G) and Ocn-Cre+Rspo2$^{f/f}$ mice (F,H), respectively, are also

35

shown. Similar to the microCT analysis, targeted mice had decreased trabecular BV/TV primarily due to a corresponding decrease in trabecular thickness, though there is a small but significant reduction in the trabecular number as well (Figures 2.7I-K). Consistent with this, the bone surface to bone volume ratio was increased in Ocn-Cre+Rspo2[f/f] mice (Figure 2.7L). However, while the total number of osteoblasts was reduced in the targeted animals, the number of osteoblasts per bone surface was not different between groups (Figure 2.7M). Additionally, we measured the interlabel distance between the two fluorescent bone labels to calculate the mineral apposition rate. The mineral apposition rate was significantly decreased in the Ocn-Cre+Rspo2[f/f] mice compared to their control littermates (Figure 2.7N). The mineralizing surface (MS/BS) was calculated by measuring the fluorescently single- and double-labeled surfaces, and this was also not different between the groups (Figure 2.7O). The bone formation rate (BFR/BS) was calculated to assess the combined contributions of mineralizing surface and mineral apposition rate. The BFR was reduced in the Ocn-Cre+Rspo2[f/f] mice (Figure 2.7P).

Decreased progenitor cell population and mineralization of BM-MSC from the conditional knockout model

Finally, bone marrow-derived MSC (BM-MSC) were isolated from WT and Ocn-Cre+Rspo2[f/f] mice for analysis of osteoblastogenesis and progenitor population. BM-MSC from targeted mice showed decreased mineralization as measured by Alizarin Red S staining (Figures 2.8A-B). However, similar to cells isolated from Rspo2[Ftl] mice, there was no difference in ALP staining (data not shown). The total mesenchymal progenitor pool and the pre-osteoblasts were evaluated using colony forming unit-fibroblast (CFU-F) and CFU-AP, respectively. Ocn-Cre+Rspo2[f/f] mice at 1-month of age showed approximately a 50% decrease in both CFU-F and

36

the percent of cells that were CFU-ALP-positive (Figures 2.8C-D). Similarly, at 3-months of age

Ocn-Cre+Rspo2$^{f/f}$ mice showed a 33% decrease in progenitor cell colonies, and a 20% decrease

in the percentage of ALP-positive progenitor colonies (Figures 2.8E-F).

2.4 DISCUSSION

The Wnt signaling pathway is important in bone development, osteoblastogenesis, and

bone maintenance and remodeling, making it a popular target for research on bone anabolic

agents. However, differential modulation of the pathway by specific ligands and cofactors, such

as R-spondins, is not well characterized. Here, we have investigated the role of the Wnt agonist

Rspo2 in osteoblastogenesis and in postnatal bone to elucidate its contribution to these

processes. We utilized Rspo2-null limb bud progenitor cells isolated from Rspo2^{ftl} mice for in

vitro investigation. We also developed a novel Rspo2 conditional knockout mouse model for

specific deletion of Rspo2 in mature osteoblasts.

Rspo2-null limb bud progenitor cells have decreased osteoblastogenesis and

mineralization, with corresponding alterations in osteogenic gene expression profile that was

somewhat surprising. Osx-null mice do not form any bone, yet even the very low Osx expression

seen here is sufficient for in vitro differentiation (Nakashima et al., 2002). Furthermore,

downstream osteogenic genes such as BSP have expression levels similar to WT cells. Moreover,

while Ocn is decreased initially, its expression reaches levels similar levels to WT cells at later

time points in osteoblastogenesis. The combination of these data suggests that there is a

mechanism for bone formation without significant Osx expression, and that there is

transcriptional regulation that allows downstream genes to be expressed at normal levels.

Consistent with this, Lrp5 knockout calvarial osteoblasts had no change in the expression of

37

Runx2, but did have a significant decrease in the expression of Osx (Riddle et al., 2013). They also had decreased mineralization with no change in ALP staining, as we observed in the both the Rspo2-null limb bud progenitor cells and BM-MSC. Comparatively, Lrp6 knockout calvarial osteoblasts had reductions in both mineralization and ALP staining, as well as moderate decreases in the expression of Runx2, Osx, and Ocn, suggesting an even earlier and more sustained role for Lrp6 in osteoblastogenesis (Riddle et al., 2013). Clearly, the osteoblast-specific Rspo2 knockout shares many of these characteristics, which could possibly be due to modulation of both Lrp5 and Lrp6 levels at the membrane. In this work we have not attempted to evaluate how Rspo2 may modulate Lrp5 and/or Lrp6 specifically.

In vivo, osteoblast-specific Rspo2 knockout resulted in a decrease in overall body mass and femur length. Via microCT analysis, we identified significant reductions in the trabecular bone volume fraction, trabecular thickness, and trabecular number, with modest reductions in cortical bone mass at the 3 month timepoint. The reduced bone mass is most pronounced at the earlier timepoints (1 and 3 months of age), corresponding to the periods of highest growth and peak trabecular bone mass in mice. By 6 months, the differences in trabecular bone have lessened, and the cortical bone is no longer significantly different from WT littermates. Bending analysis reflected the significant differences seen in the cortical bone on microCT at 1 and 3 months of age. At 6 months of age, male mice had significant reductions in the maximum load force and bending stiffness, while the microCT data only showed a trend toward reduction.

Our histomorphometry data show that Rspo2 deficiency in osteoblasts results in decreased mineral apposition in despite of similar numbers of osteoblasts per bone surface, suggesting a deficiency in osteoblast activity. Further supporting this, while the mineralizing surface fraction is similar to wild-type animals, the decreased bone formation rate confirms a

38

decreased overall production of new bone. This corresponds to our in vitro mineralization data for both the Rspo2-null limb bud progenitor cells (Figure 2.1) as well as BM-MSC from the targeted Rspo2^{floxed} mice (Figure 2.8). Interestingly, the progenitor cell population in the bone marrow of our Ocn-Cre+Rspo2$^{f/f}$ mice showed decreases in both total colony number and percentage of ALP-positive colonies by CFU-F analysis. Despite this decreased osteoblastogenesis potential, the mice have similar numbers of osteoblasts per bone surface compared to WT littermates, suggesting that this diminished osteoblastogenesis is still sufficient to produce osteoblasts during growth. Whether this progenitor pool and differentiation potential are still adequate during aging or in the face increased demands such as ovariectomy or fracture remains to be investigated. Overall, Rspo2 deficiency causes a decrease in osteoblastogenesis and mineralization both in vitro and in vivo, and this deficiency leads to decreased bone mass in mice.

The decreased bone length seen here presents an intriguing question, given that the length of the long bones is primarily determined by appropriate function of the growth plate. The Osteocalcin promoter used to express Cre in this model is also expressed in late hypertrophic chondrocytes, which may provide a mechanism for abnormality in the growth plate (Zhang et al., 2002). Deficiency of Rspo2 in chondrocytes has been reported to decrease chondrocyte proliferation, but differences in protein expression in the hypertrophic zone were not noted (Takegami et al., 2016). However, canonical Wnt signaling is known to affect progression of chondrocytes through the growth plate, and, consistent with this, Lrp5 knockout mice also have shortened femoral length (Kato et al., 2002). Given that hypertrophic chondrocytes are known to transdifferentiate to osteoblasts, it is possible that the Rspo2

39

deficiency hinders the activation of the pluripotent stem cell programs required for this process (Bahney et al., 2014; Zhou et al., 2014).

The overall skeletal phenotype of the osteoblast-specific knockout of Rspo2 is consistent with that seen in other disruptions of canonical Wnt signaling in bone, specifically that of Lrp5 disruption, albeit somewhat attenuated (Gong et al., 2001; Holmen et al., 2004). Specifically, the Lrp5 knockout mouse has decreased bone mass, decreased mineral apposition rate, decreased osteoblast numbers, and decreased femoral length, all of which are similar to the phenotype seen with osteoblast-specific knockout of Rspo2 (Kato et al., 2002). Despite these post-natal effects, overall skeletal development, similar to the osteoblast-specific Rspo2 knockout reported here but in contrast to the global Rspo2 knockout, is relatively normal. When the Lrp5 knockout mouse is crossed with the Lrp6 knockout mouse to create double knockouts, skeletogenesis defects emerge similar to those seen in the Cttnb1 (Beta-catenin) and Rspo2 global knockout, although with different left/right and anterior/posterior patterns (Holmen et al., 2004; Hill et al., 2005). LRP5 and LRP6 are the transmembrane co-receptors mediating canonical Wnt signaling, along with the Frizzled receptors, and are regulated by ZNRF3 and RNF43, which are themselves inhibited by Rspo2 (Hao et al., 2012; Koo et al., 2012). Therefore, the consistency of the Ocn-Cre Rspo2-deficient phenotype with Lrp5 deficiency corroborates the hypothesis that Rspo2 modulates canonical Wnt signaling in bone likely through modulation of Lrp5 and perhaps Lrp6 receptors. While not examined, it is probable that the absence of Rspo2 produced by osteoblasts, results in decreased Lrp5/6 receptors on osteoblasts. Additional studies utilizing combined knockouts of Rspo2 with these receptors would help elucidate this interaction.

The microCT results show consistently decreased trabecular bone in the 1-, 3-, and 6-month old mice, primarily due to decreased trabecular thickness. However, the phenotype does

40

not increase in severity from 3 to 6 months. This is likely due to the fact that this is primarily a period of bone resorption therefore the defective mineralization seen in our model may be less significant during this time period (Jilka, 2013). While there are corresponding decreases in osteoclasts seen via TRAP staining, these are only sufficient to moderately attenuate the difference between the groups. This phenotype contrasts with the Wnt10b-null mouse model in which the growth rate and bone mass are normal to enhanced at 1 month of age, but progressive osteopenia develops thereafter (Stevens et al., 2010). The differences in cortical bone parameters also lessen to the point of no longer being different at 6 months of age. This may possibly be due to smaller magnitude differences and a lack of statistical power in this study; however, Wnt signaling phenotypes in bone have shown unique phenotypes depending on the signaling molecules targeted. As an example, over expression of Wnt10b increases trabecular bone, with minimal impact on cortical bone (Bennett et al., 2007). Additionally, biomechanical testing demonstrated decreased bone strength via 3-point-bending at 3- and 6-months of age, which corresponds primarily to cortical bone strength due to force application at the mid-diaphysis. Though there were no significant differences in cortical bone parameters via microCT at 6 months, the mechanical testing was able to detect differences in the bone with greater sensitivity. Further studies to age our novel model to a geriatric timepoint are needed to determine whether Rspo2-deficient mice are able to maintain their bone mass or if the phenotype becomes more severe over a longer time period. As well, investigation into the coupling of osteoblasts and osteoclasts in the face of Rspo2-deficiency may help to explain the lack of further loss of bone mass from 3 to 6 months seen here.

The decreased progenitor cell and pre-osteoblast populations as determined by CFU-F and CFU-AP respectively, are also somewhat unexpected given the similar numbers of

41

osteoblasts observed via histology. Disruptions of canonical Wnt signaling have been shown to decrease these parameters, such as in the Lrp5-knockout and the Wnt10b-knockout models (Kato et al., 2002; Stevens et al., 2010). However, high levels of expression of stabilized beta-catenin decreased the number of CFU-F colonies, while lower levels of expression enhanced the proliferation of MSC thereby increasing these numbers (Kim et al., 2015). In another study, addition of Wnt3a, a stereotypically canonical Wnt ligand, increased both total number and percentage of ALP-positive colonies, while addition of Wnt5a, a stereotypically noncanonical Wnt ligand, had no effect in this assay (Baksh and Tuan, 2007). Clearly the tuning of specific Wnt ligands is critical to Wnt signaling's ultimate effects on progenitor cell renewal, proliferation, and differentiation. In our mouse model, the clear reduction in progenitor cell population does not appear to affect the number of osteoblasts present on the bone surface by histomorphometric analysis, which further suggests that the mechanism of the decreased bone mass is due to reduced functionality of the osteoblasts rather than a lack of progenitor cells or a decreased potential to differentiate. However, given the reduced progenitor cell population, it is conceivable that mice with osteoblast deficiency in Rspo2, would have a reduced regenerative capacity when challenged with a fracture or segmental defect, and may lose bone more quickly when challenged by aging or ovariectomy.

Together, our data indicate that Rspo2 modulates osteoblastogenesis and mineralization, both in vitro and in vivo. Rspo2-deficiency leads to decreased mineral apposition and bone formation rates, and thus to fewer and smaller trabeculae and decreased overall bone mass. Additionally, Rspo2-deficiency results in decreased bone strength resulting from changes in cortical bone. This specific phenotype is similar to other models that perturb the canonical Wnt signaling pathway, particularly those that disrupt receptors Lrp5 and Lrp6, supporting the

canonical Wnt signaling pathway as the primary mechanism of Rspo2activity in osteoblasts. However, the clear differences between our model and previous models that disrupt specific Wnt ligands suggest that Rspo2 modulates the receptors that integrate the signal from many Wnt ligands rather than tuning one specific Wnt ligand-mediated signal. Given that the reduction in bone mass is more modest compared to some of the other models that disrupt Wnt signaling, this could be beneficial as an option to more carefully tune the activity of osteoblasts therapeutically. In summary, we have established Rspo2 as an important modulator of bone mass via its regulation of osteoblast function in postnatal bone.
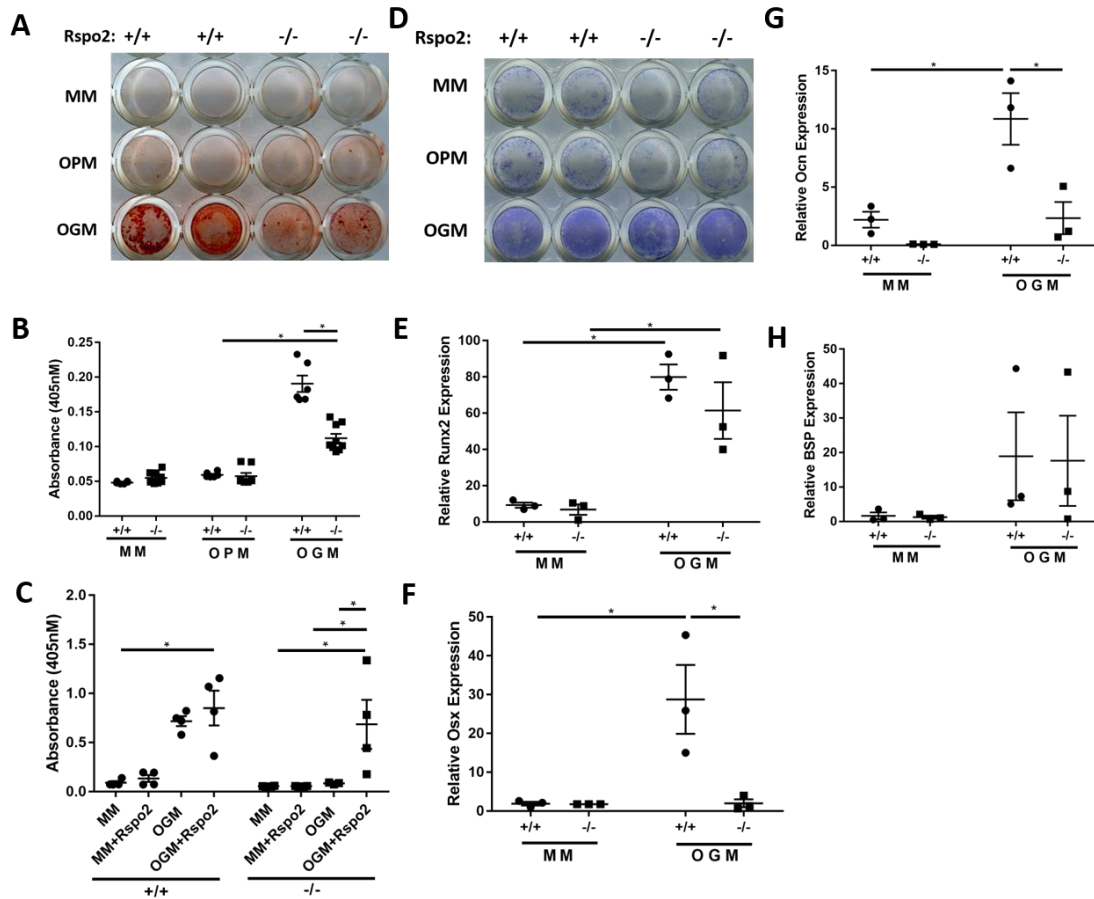
Figure 2.1. R-spondin-2 Null mesenchymal progenitor cells undergo decreased osteoblastogenesis. A. Alizarin red S staining of representative wells from in vitro osteogenesis assay after 10 days. MM = Maintenance media, OPM = osteopermissive media with β-glycerophosphate and ascorbic acid-2-phosphate, OGM = osteogenic media with OPM and 2.5nM rhBMP-6. B. Overall quantification of Alizarin Red S staining of osteogenesis at 10 days, as shown in panel A. C. Quantification of osteogenesis at 15 days with addition of recombinant hRSPO2 (10nM). D. Alkaline Phosphatase (ALP) staining of similar osteogenesis assay at 5 days. E. Relative Runx2 expression after 5 days of osteogenesis in vitro. F. Relative Osterix expression after 5 days of osteogenesis in vitro. G. Relative Osteocalcin expression after 10 days of osteogenesis in vitro. H. Relative Bone Sialoprotein (BSP) expression after 5 days of osteogenesis in vitro. (n= 3 cell lines from individual animals, assay performed in triplicate), * indicates $p < 0.05$.
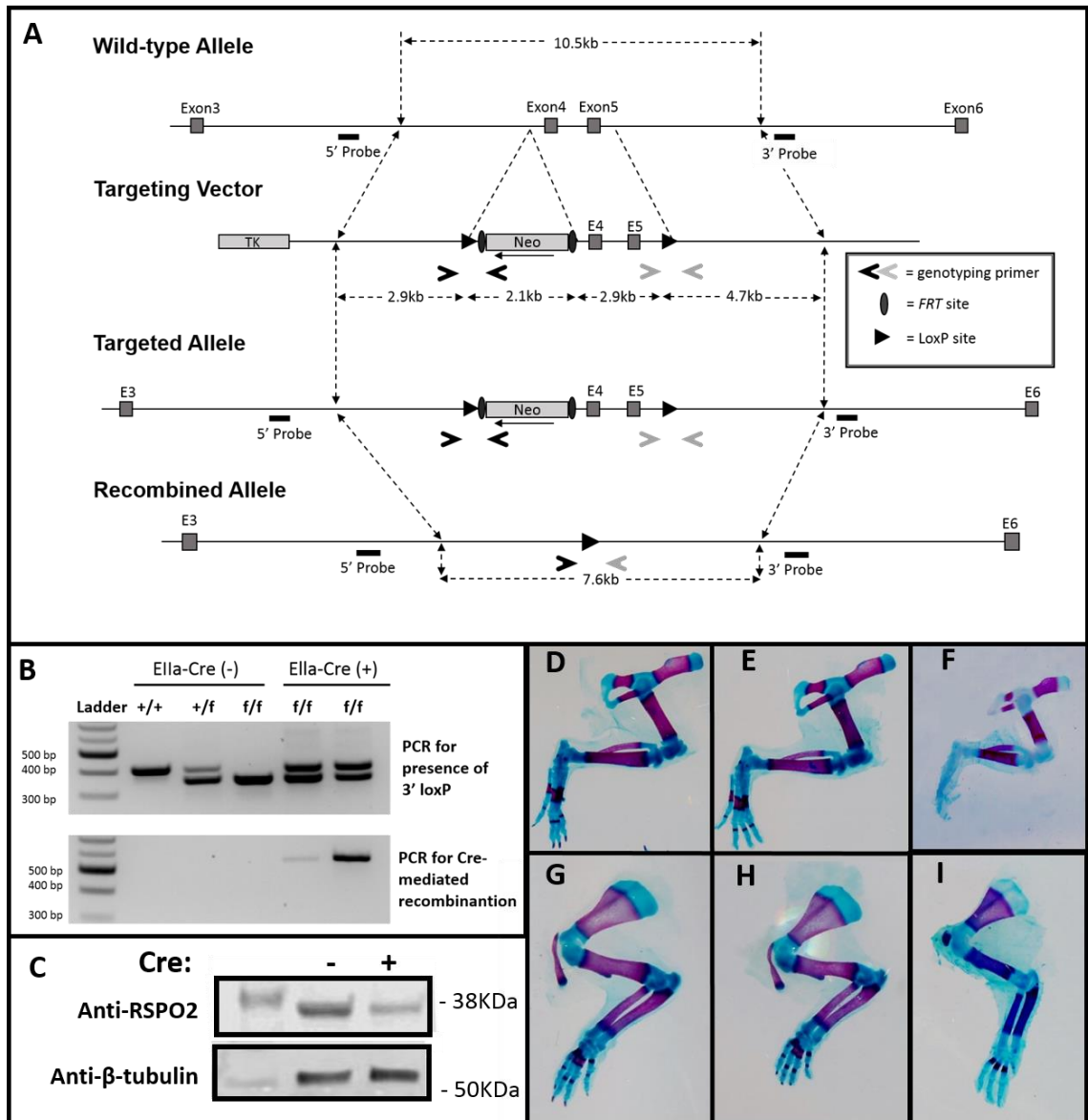
44

Figure 2.2. Generation of R-spondin-2 Conditional Allele. A. Map of the genomic region of exons 3 to 6 of Rspo2 in alignment with the targeting vector with exons 4 and 5 flanked by loxP sites (triangles), as well as the addition of a neomycin cassette flanked by FRT sites. The targeted allele after homologous recombination follows, which is then in alignment with the final recombined allele after Cre recombination of the loxP sites. Genotyping primers are shown as open arrows (Primer set A dark-grey; Primer set B, light-grey), and Southern blot probes are denoted. B. Genotyping of mice with primers Rspo2-FloxB-for, Rspo2-FloxB-rev, and Rspo2-FloxA-For. C. Western blot of BM-MSC harvested from mice of denoted genotypes. Pelvic limbs (D-F) and thoracic limbs (G-I) from embryonic skeletal preparations. Limbs from representative WT embryos shown in D, G. E, G from most minorly affected EIIa-Cre+Rspo2$^{f/f}$ embryos. F, H from more severely affected embryos. D-E,G-I from E18.5 embryos, F from E16.5 embryo.
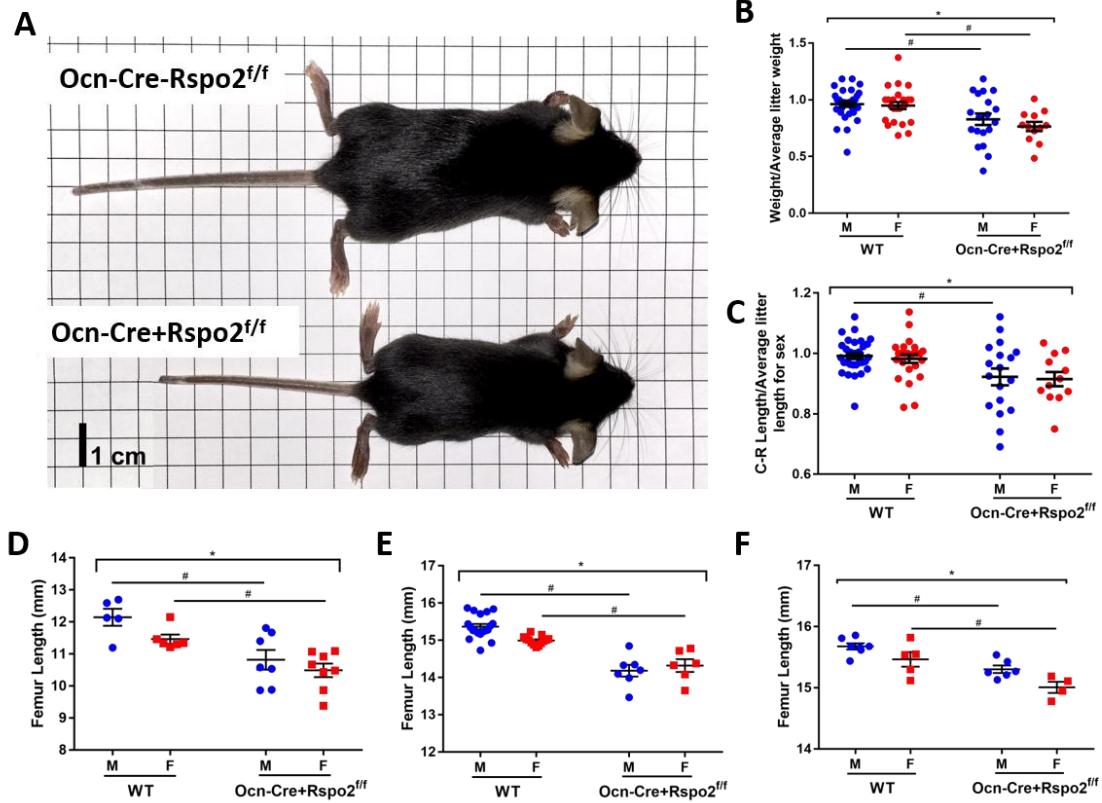
Figure 2.3. Osteoblast-specific Rspo2 knockout has decreased body size. A. Comparison of WT (top) vs. Ocn-Cre+Rspo2^f/f (bottom) mice at 3 weeks. B. Normalized weights of 3-week-old mice. C. Normalized Crown-Rump length of 3 weeks old mice. D. Femur length of 1-month-old mice. E. Femur length of 3-month-old mice. F. Femur length of 6-month-old mice. *indicates p<0.05 for genotype groups. # indicates p<0.05 for genotypes within sex. Blue circles = males; Red squares = females.

Figure 2.4. Targeted mice have decreased trabecular and cortical bone parameters. A-H. Micro-Computed Tomography (uCT) of femurs from 3-month-old mice. Femurs were analyzed for bone volume fraction (A), trabecular number (B), trabecular thickness (C), trabecular bone mineral density (D), cortical bone mineral density (E), cortical thickness (F), periosteal perimeter (G), and endosteal perimeter (H) I-J. Three dimensional reconstructions of mid-diaphyseal cortical bone (I) and metaphyseal trabecular bone (J) from representative 3-month old mice. 3-point bending of femurs from 3-month-old mice. Femurs were analyzed for (K) Maximum Load

and (L) Bending Stiffness. *indicates p<0.05 for genotype groups. # indicates p<0.05 between genotypes within sex.
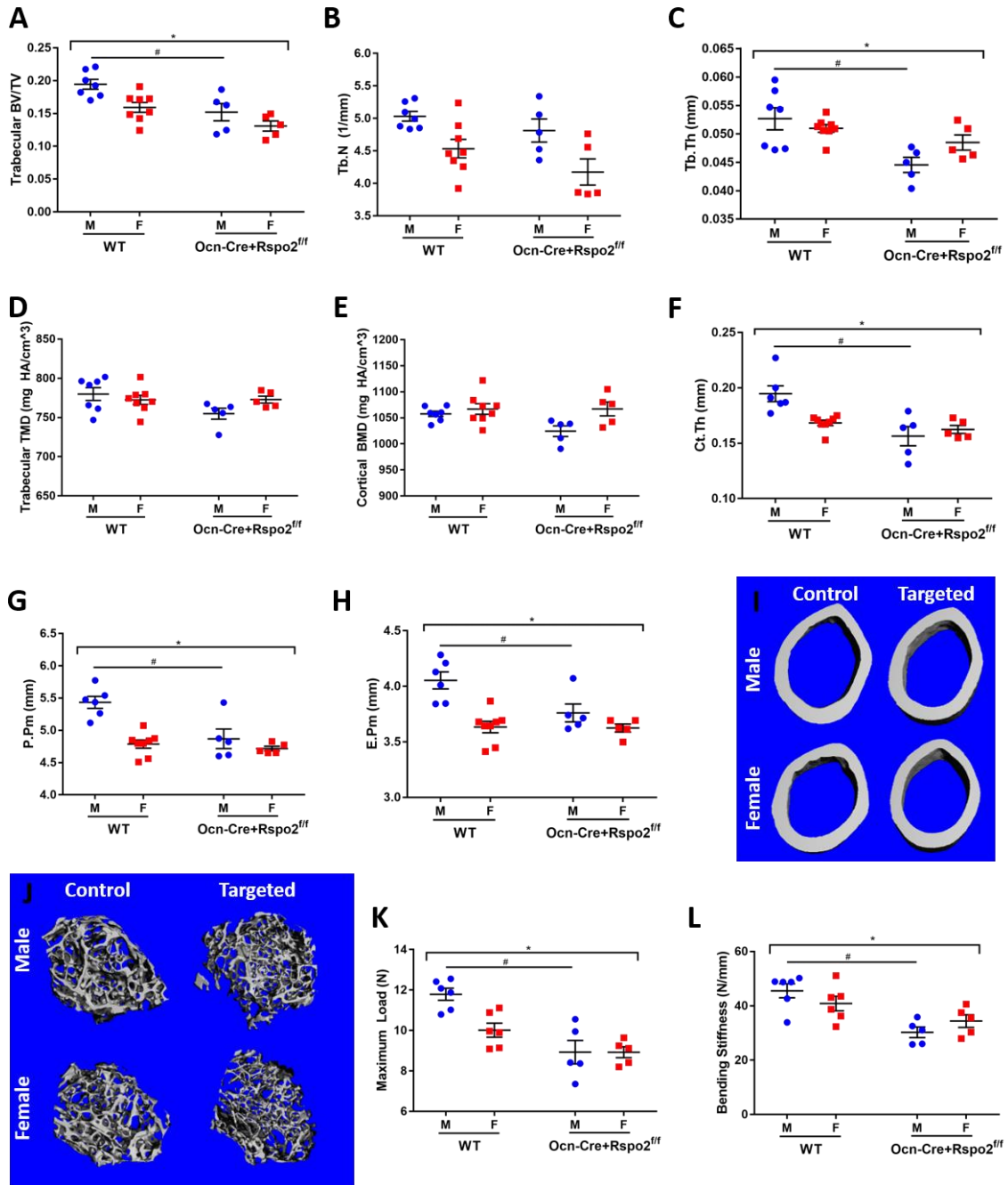
Figure 2.5. Targeted mice have decreased trabecular and cortical bone parameters. A-H. Micro-Computed Tomography (uCT) of femurs from 1-month-old mice. Femurs were analyzed for bone volume fraction (A), trabecular number (B), trabecular thickness (C), trabecular bone mineral density (D), cortical bone mineral density (E), cortical thickness (F), periosteal perimeter (G), and endosteal perimeter (H) I-J. Three dimensional reconstructions of mid-diaphyseal cortical bone (I) and metaphyseal trabecular bone (J) from representative 1-month old mice. 3-point bending of femurs from 1-month-old mice. Femurs were analyzed for (K) Maximum Load

and (L) Bending Stiffness. *indicates p<0.05 for genotype groups. # indicates p<0.05 between genotypes within sex.
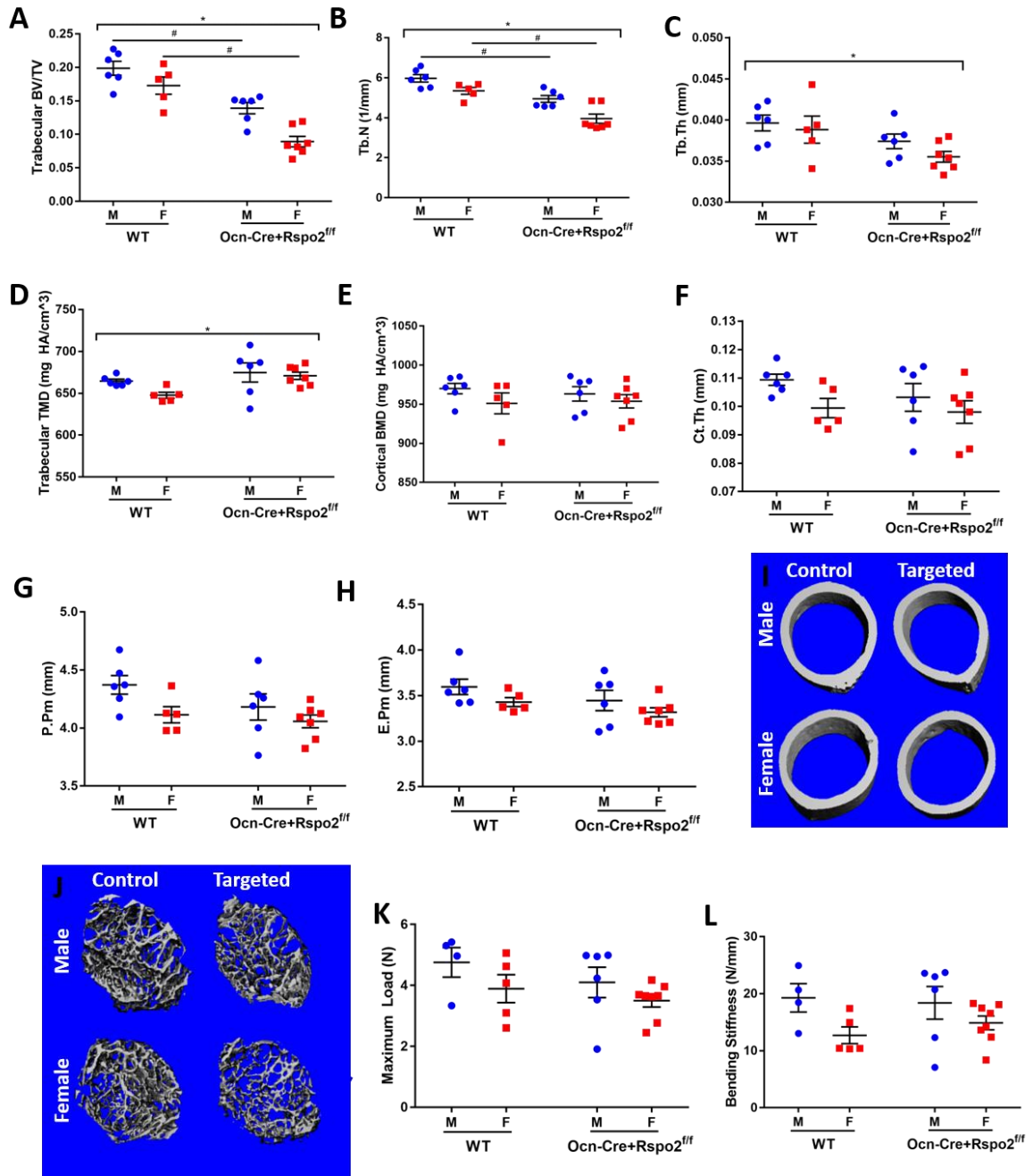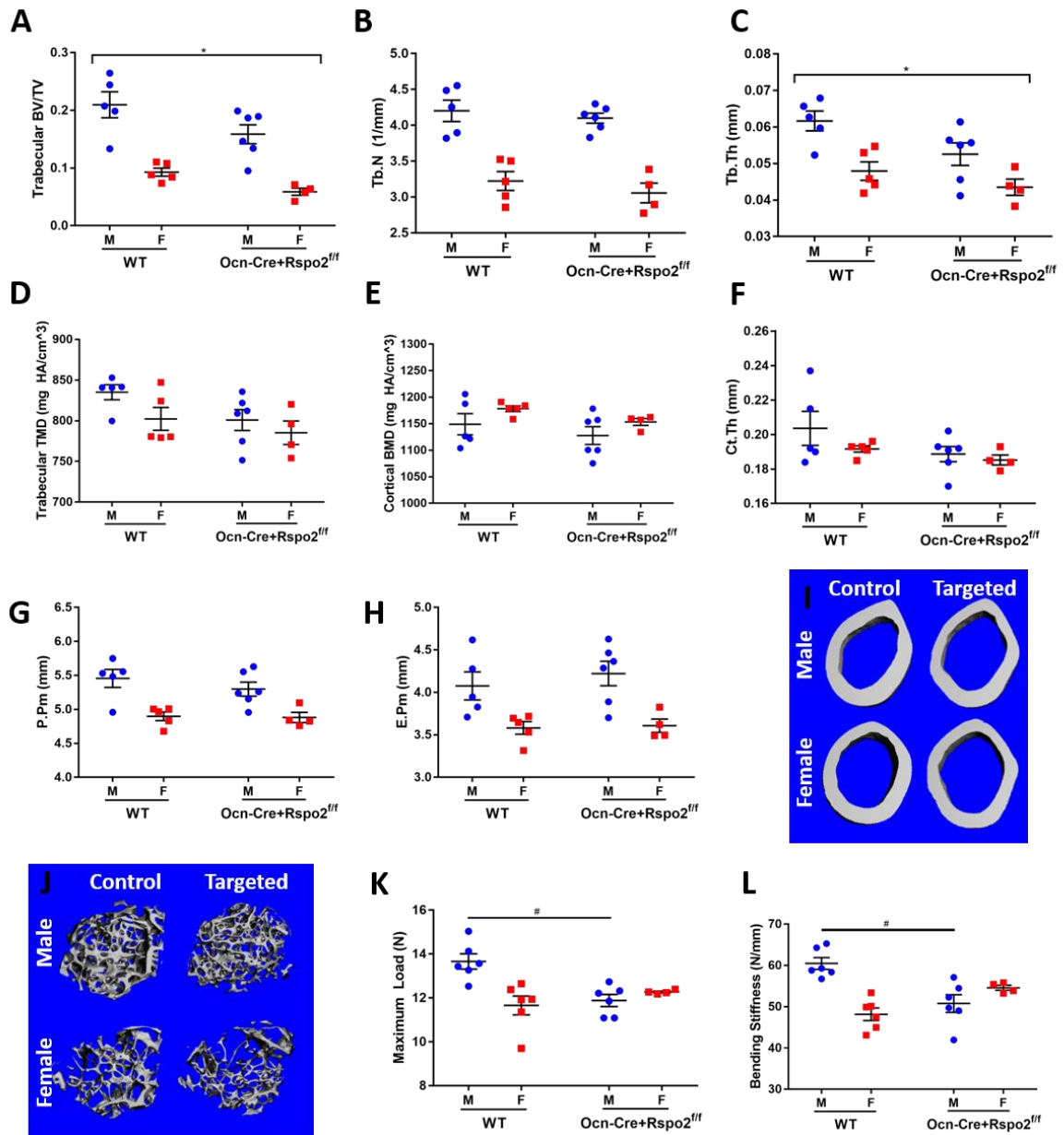
Figure 2.6. Targeted mice have decreased trabecular and cortical bone parameters. A-H. Micro-Computed Tomography (uCT) of femurs from 6-month-old mice. Femurs were analyzed for bone volume fraction (A), trabecular number (B), trabecular thickness (C), trabecular bone mineral density (D), cortical bone mineral density (E), cortical thickness (F), periosteal perimeter (G), and endosteal perimeter (H) I-J. Three dimensional reconstructions of mid-diaphyseal cortical bone (I) and metaphyseal trabecular bone (J) from representative 6-month old mice. 3-point bending of femurs from 6-month-old mice. Femurs were analyzed for (K) Maximum Load and (L) Bending Stiffness. *indicates p<0.05 for genotype groups. # indicates p<0.05 between genotypes within sex.
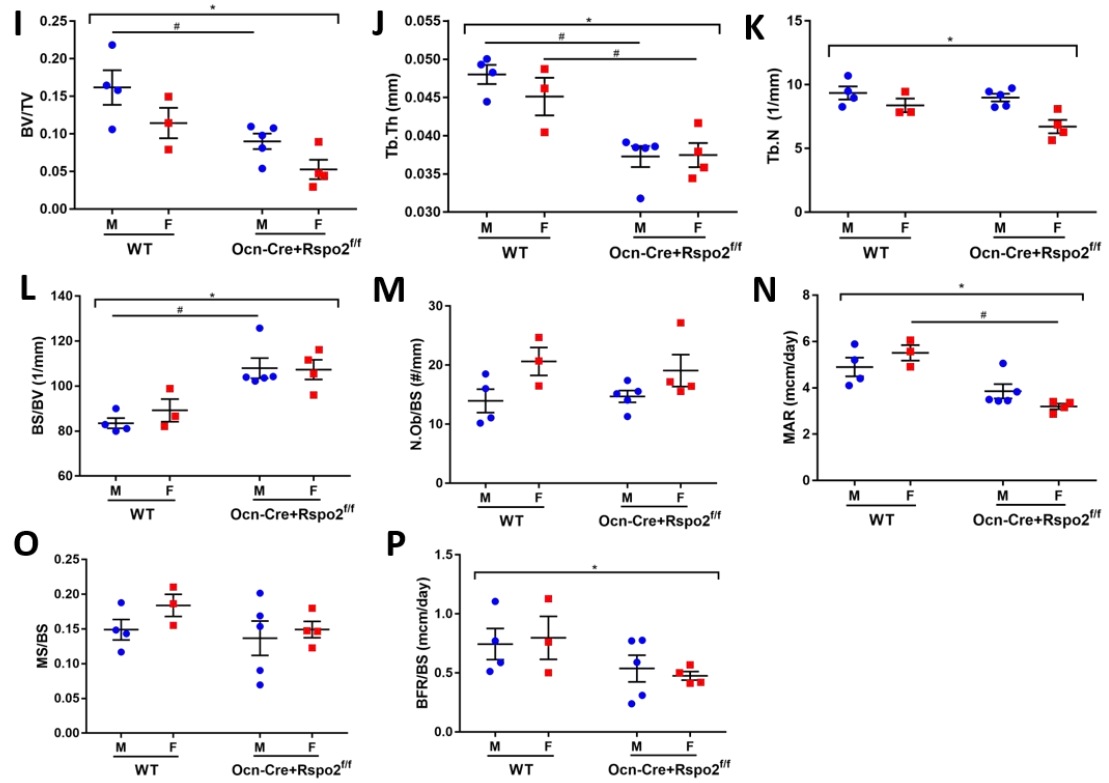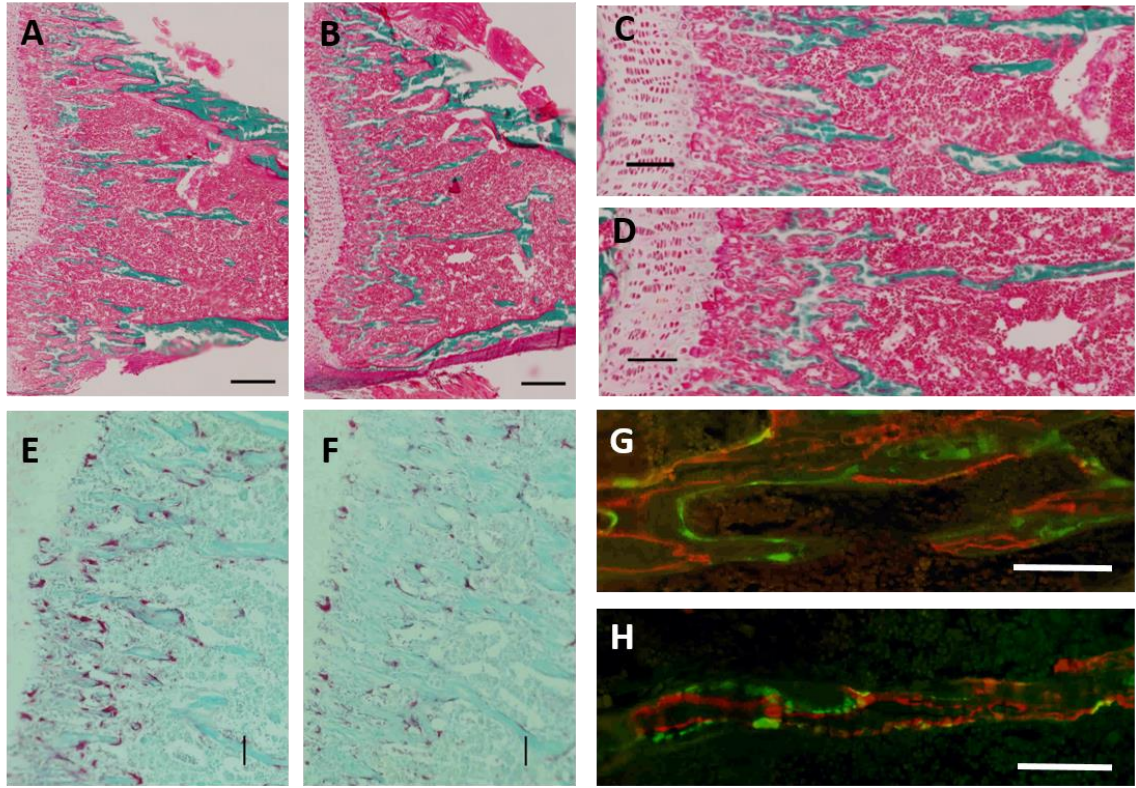
Figure 2.7. Osteoblast-Specific Knockout of Rspo2 results in decreased mineralization and bone mass. A-D. Histologic sections of the proximal tibia of representative 1-month-old mice stained with Goldner's Trichrome. A,C. WT control mice. B,D. Ocn-Cre+Rspo2$^{f/f}$ mice. E-F. TRAP staining of representative histologic sections of 1-month-old mice. E. WT control mouse. F. Ocn-Cre+Rspo2$^{f/f}$ mouse. G,H. Double-labeled bone sections from representative 1-month-old mice. G. WT control mouse. H. Ocn-Cre+Rspo2$^{f/f}$ mouse. I-L. Histomorphometric parameters from 1-month-old mice. Tibias were analyzed for bone volume fraction (I), trabecular thickness (J), trabecular number (K), bone surface (L), osteoblasts per bone surface (M), mineral apposition rate (N), mineralizing surface (O), bone formation rate (P). Scale bars are 200uM in A,B; 166uM in C,D; 100uM in E-H. *indicates $p<0.05$ for genotype groups. # indicates $p<0.05$ for different genotypes within sex. Blue circles = male; red squares = females.
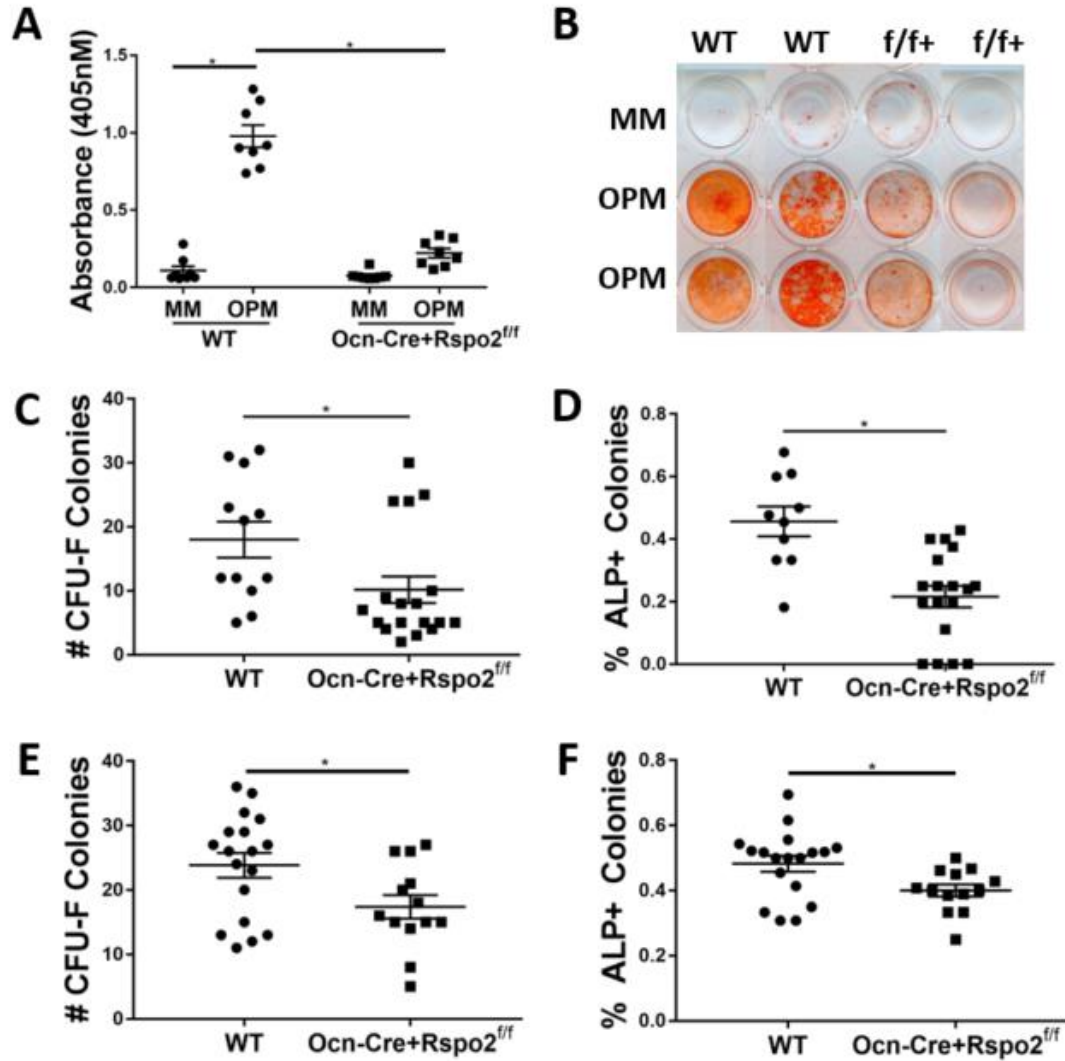
Figure 2.8. Osteoblast-specific Rspo2 knockout has decreased progenitor cells and BM-MSC mineralization. A. Quantification of Alizarin red S staining of 10 day osteogenesis with BM-MSC from 1-month-old mice. MM = Maintenance Media, OPM = Osteopermissive media with β-glycerophosphate and ascorbic acid-2-phosphate, OGM = osteogenic media with OPM and 2.5nM rhBMP-6. B. Alizarin Red S staining of representative wells after 10 days of osteogenesis. C. Quantification of total number of CFU-F colonies from bone marrow flushed from 1-month-old mice. D. Quantification of percent ALP-positive colonies from bone marrow flushed from 1 month-old mice. E. Quantification of total number of colonies from bone marrow flushed from 3-month-old mice. F. Quantification of percent ALP-positive colonies from bone marrow flushed from 3-month-old mice. *indicates $p < 0.05$.

54

	f/+; Cre-	f/+; Cre+	f/f; Cre-	f/f; Cre+
Frequency	0.25	0.17	0.17	0.42
N	6	4	4	10

Table 1. Genetic frequency of P18.5 pups resulting from EIIa-Cre-Rspo2$^{f/f}$ x EIIa-Cre+Rspo2$^{f/+}$ matings.

	f/+; Cre-	f/+; Cre+	f/f; Cre-	f/f; Cre+
Frequency	0.36	0.29	0.36	0
N	5	4	5	0

Table 2. Genetic frequency of P21 pups resulting from EIIa-Cre-Rspo2$^{f/f}$ x EIIa-Cre+Rspo2$^{f/+}$ matings.

55

CHAPTER 3: DISCUSSION

3.1 SUMMARY

The Wnt agonist Rspo2 has an established role in skeletal development, and here we present its significant role in osteoblasts in postnatal bone. Canonical Wnt signaling is one of the most studied pathways in bone due to its osteoanabolic effects through both enhancement of osteoblastogenesis and modulation of osteoblasts in remodeling. The pathway was originally implicated when loss-of-function mutations in Lrp5 were found to cause osteoporosis pseudoglioma syndrome, and a substantial body of research has been generated since this original finding (Gong et al., 2001; Monroe et al., 2012). In fact, the first Wnt-related therapeutic for osteoporosis is slated to gain FDA approval this year. Despite this great progress, the precise control of osteoblastogenesis and bone accrual mediated by Wnts is still largely unknown, with different ligands and different levels of signaling activity leading to unexpected and opposing effects. Furthermore, while there are many studied pathway inhibitors, there have few positive co-modulators of the pathway identified, making the R-spondins unique in their action.

Considering the positive regulation of the canonical Wnt pathway by the R-spondins and the established role of Rspo2 in skeletal development, we hypothesized that it may also have a positive regulatory role in osteoblastogenesis and bone accrual. Previous findings from our laboratory revealed that overexpression of Rspo2 in pre-osteoblasts enhanced osteoblastogenesis and mineralization (Friedman et al., 2009). Here, I utilized limb bud progenitor cells from Rspo2 knockout mice to assess in vitro osteoblastogenesis in Rspo2-null cells. However, the perinatal lethality of the global Rspo2-knockout mouse model precluded the study of Rspo2 in postnatal bone in vivo. To address this, I created a novel conditional Rspo2-knockout mouse, and specifically disrupted the Rspo2 expression in osteoblasts via expression

56

of Cre-recombinase driven by the Osteocalcin promoter. This is the first report of the autocrine action of Rspo2 in osteoblasts.

Here, we show that Rspo2 deficiency causes defects in osteoblastogenesis, mineralization, and bone accrual. Rspo2-null osteoblasts undergo less mineralization than wild-type cells, though their levels of ALP staining are similar. These Rspo2-null cells also have decreased expression of Osterix and Osteocalcin compared to wild-type cells, though levels of Runx2 and BSP are unaffected. This phenotype can be rescued by the addition of recombinant RSPO2 to the media. Altogether, Rspo2-null osteoblasts do have the ability to mineralize, as seen by Alizarin red S staining, and do so progressively over time. However, this mineralization is defective and never reaches wild-type levels.

Rspo2-deficiency in osteoblasts in vivo also leads to a phenotype of decreased mineralization. This was investigated through the development of a novel conditional mouse model of Rspo2 knockout. When mice with loxP sites floxing exons 4 and 5, are crossed to the pan-expressing Cre mouse, EIIa-Cre, for whole-body recombination, the offspring recapitulate the limb malformation phenotype and perinatal lethality phenotypes of the global Rspo2-knockout. These mice were also crossed with Osteocalcin-Cre mice for specific recombination in the osteoblasts. Mice with Rspo2-deficient osteoblasts are smaller than their littermates, by both weight and crown-rump length. At 1, 3, and 6 months of age, their femurs are significantly shorter than their wild-type littermates. At all three timepoints investigated, these mice have decreased trabecular bone volume fraction, characterized by thinner trabeculae. At the 1 month timepoint there are also fewer trabeculae. Cortical bone is reduced in mice with Rspo2-deficient osteoblasts at 3 months, and the bones show reduced mechanical strength in bending. Non-

57

statistically significant geometric differences persist at 6 months of age, and the changes are reflected in a continued reduction in mechanical strength of the Rspo2-deficient mice.

Histomorphometric analysis revealed differences in bone volume fraction and trabecular thickness at 1 month of age similar to the findings with microCT. Additionally, these Ocn-Cre+Rspo2$^{f/f}$ mice have a decreased bone formation rate (BFR). This decreased BFR corresponds to a decreased mineral apposition rate, as the mineralizing surface ratio is not altered in the mice with Rspo2-deficient osteoblasts. When BM-MSC are harvested from these mice and stimulated to undergo osteoblastogenesis in vitro, they produce less mineral but have similar ALP staining. Additionally, when the progenitor cell population in the marrow is measured via CFU-F analysis, these mice have decreased total numbers and ALP-positive fraction of colonies produced. Altogether, these studies show that Rspo2 is critical for normal osteoblastogenesis and mineralization, and that when this deficiency occurs in vivo, there is a decreased bone formation rate that results in a decrease in total bone.

3.2 DISCUSSION

The role of R-spondin-2 in osteoblastogenesis of limb bud mesenchymal progenitor cells

The differentiation and function of osteoblasts is critical to the formation and maintenance of bone, as discussed in Chapter One. Alterations in osteoblast and osteoclast activities disrupts remodeling homeostasis, causing alterations in bone mass and structure such as osteoporosis. Determining methods in which osteoblasts and osteoclasts can be modulated to re-establish this balance, or even shifting the balance in the favor of osteoblast-mediated re-building of bone, is critical for the development of novel therapeutics for conditions of low bone

mass. Fundamental to this is an understanding of the signaling pathways and key factors involved in osteoblast differentiation and function.

Canonical Wnt signaling has been established as a positive regulator of both osteoblastogenesis and osteoblast activity (Monroe et al., 2012). Furthermore, R-spondins have been identified as agonists of Wnt signaling, and our laboratory previously showed that enhanced Rspo2 expression in pre-osteoblasts increased their mineralization in vitro (Friedman et al., 2009). In Chapter Two, we utilized limb bud mesenchymal progenitor cells from Rspo2-knockout mice to address the question of the requirement of Rspo2 for osteoblastogenesis and mineralization. Given that R-Spondins are thought to enhance Wnt signaling by increasing the Wnt co-receptors at the cell surface, we hypothesized that some signaling would still occur in these cells, and thus they would still mineralize to some extent, albeit less efficiently than wild-type cells. The Rspo2-null mesenchymal progenitor cells (MPC) had decreased mineralization at all timepoints assessed, confirming this hypothesis. Their ALP staining was similar to that of wild-type cells though, suggesting that early osteoblastogenesis may not be altered with Rspo2-deficiency.

The multi-step process of the production of bone matrix may provide some insight into potential defects caused by Rspo2-deficiency during osteoblastogenesis. Initially, there is deposition of organic extracellular matrix, which consists primarily of type-I collagen, proteoglycans (including decorin and biglycan), and some non-collagen proteins such as osteocalcin, osteonectin, bone sialoprotein, and osteopontin. Next, mineralization occurs near the ends of aligned collagen fibrils. Mineralization occurs in two stages: a vesicular stage and a fibrillar stage. During the vesicular stage, ALP releases inorganic phosphate from phosphate-containing compounds in the vesicles. Additionally, proteoglycans in the matrix are degraded,

59

releasing calcium, which is transported into the vesicles through annexin channels. The concentrated calcium and phosphate ions, coordinated with other proteins and phospholipids, then nucleate and form hydroxyapatite crystals, which then grow and eventually rupture the vesicle and thus beginning the fibrillar stage (Clarke, 2008; Florencio-Silva et al., 2015). Given the normal ALP levels in Rspo2-deficient osteoblasts, along with the decreased mineralization, it is likely that another component of the mineralization pathway is disrupted. It is possible that this could be a defect in the deposition of type 1 collagen, leading to decreased sites of initial mineral nucleation. As well, alterations in the calcium- and phosphate- binding proteins or components of the nucleation complex in the vesicles could lead to decreased mineralization. Additionally, alterations in the annexin channels could lead to decrease calcium concentration in the vesicular microenvironment, resulting in decreased hydroxyapatite crystal nucleation.

In order to mineralize, the MPC require an osteogenic growth factor. Typically, we use recombinant BMP6 for this purpose, but since R-spondins are known to stimulate both canonical and noncanonical signaling, it is important to consider how canonical and noncanonical signaling may affect the Rspo2-null MPC osteoblasts differentially. Wnt ligands Wnt3a and Wnt5a were used as growth factors to stimulate osteoblastogenesis in the MPC. While Wnt3a is an established canonical Wnt ligand, Wnt5a is commonly described as a noncanonical Wnt ligand, though it is known that the specificity for stimulation of one specific Wnt signaling pathway is not as strong as was once assumed. Although ALP staining was still similar in WT and Rspo2-null MPC treated with BMP6, Rspo2-null MPC treated with Wnt3a or Wnt5a had increased ALP staining compared to WT cells in the same conditions (Figure 3.1). Moreover, the ALP staining resulting from Wnt3a vs Wnt5a was similar within the same cell line. However, similar to stimulation with BMP6, Rspo2-null MPC had decreased levels of

60

mineralization compared to WT cells when stimulated with either Wnt ligand (data not shown). This discordance between these markers of two stages of osteoblastogenesis in the Rspo2-null cells is intriguing. Since ALP expression does decrease as osteoblastogenesis progresses in some cells, it is possible that this data is reflective of the Rspo2-null cells being retarded in their progression through osteoblastogenesis. However, these cells had increased staining compared to the wild-type cells at both 5 and 7 days. It is therefore more likely that these cells have decreased overall Wnt signaling due to the lack of Rspo2, and are not maintained in the progenitor cell state as efficiently, thus causing them to initiate osteoblastogenesis. Wnt signaling is also involved in downstream stages of differentiation to mature osteoblasts, and this is also likely hindered, causing the decreased mineralization observed.

Another role established for canonical Wnt signaling in MPC is the concurrent inhibition of adipogenic cell fates and promotion towards the osteogenic fate. In contrast, noncanonical Wnt signaling is reported to increase adipogenesis. Moreover, the reciprocal relationship between adipogenesis and osteogenesis is commonly cited, mirroring the frequent reciprocal relationship between canonical and noncanonical Wnt signaling (Keats et al., 2014). Given this, and the phenotype of decreased osteogenesis that we established, we hypothesized that Rspo2-null MPC would undergo significantly more adipogenesis than WT MPC. However, when stimulated to undergo adipogenesis, Rspo2-null MPC produced significantly less lipid than WT MPC, as seen by quantification of Oil Red O staining of cells (Figure 3.2). The puzzling lack of the reciprocal relationship here is likely due to one of two scenarios: i) cells are maintained in a progenitor cell state, or ii) differentiation is incomplete. When considering this data with the increased ALP staining observed with stimulation by Wnt ligands, it seems most likely that Rspo2-deficient cells are perhaps 'stalled' in osteoblastogenesis. It is possible that they are even

61

more stimulated to undergo osteoblastogenesis, rather than adipogenesis, given that they show both reductions in Oil Red O staining and increases in ALP staining. In this scenario, as mentioned above, it is likely that the decrease in Wnt signaling results in a lack of maintenance of the progenitor cell population.

We also measured the relative osteogenic gene expression profiles of the Rspo2-null MPC compared to the WT MPC. The master regulator of osteoblastogenesis is reported to be the transcription factor, Runx2. Without expression of Runx2, no bone is formed (Otto et al., 1997). Both the Rspo2-null and WT MPC showed induction of Runx2 with stimulation of osteoblastogenesis in vitro, with similar levels of expression. It could be expected that, given the above findings, expression of Runx2 would be higher in the Rspo2-null cells. However, there was not a difference observed here at the gene expression level. A possible explanation for this is that Runx2 is known to be post-transcriptionally regulated, so Runx2 levels could be enhanced without changes in gene expression.

The next major transcriptional regulator of osteoblastogenesis is the transcription factor, Osterix. In Osx-null mice, no bone matrix is deposited via endochondral or intramembranous ossification, though the hypertrophic cartilage is calcified in contrast to the Runx2-null mice. The Rspo2-null MPC show reduced expression of Osx at all timepoints compared to the WT MPC. Given this, it is somewhat surprising that these Rspo2-deficient cells are able to mineralize in vitro, as Osx-null MPC do not mineralize in culture (Nishimura et al., 2012). Interestingly though, the Rspo2-null MPC go on to express down-stream osteogenic genes, such as Osteocalcin (initially reduced, as mentioned in Chapter 2) and BSP. This suggests that either the very low levels of Osx expression are sufficient to induce the expression of these downstream genes, or that there is a parallel pathway leading to their induction. However, this

62

downstream gene expression does provide an explanation for how the cells are able to eventually mineralize in culture. Many of the osteogenic genes contain Runx2- binding sites in their promoters, which are reported to work in concert with Osx for gene expression; however, it is possible that other factors are also able to serve this role, such as other Sp-family transcription factors (Thirunavukkarasu et al., 2002; Zhang et al., 2010). Moreover, consistent with the gene expression pattern of Rspo2 null cells, is the osteogenic gene expression seen in Lrp5- and Lrp6-null osteoblasts. These cells have reduced levels of Osx expression, but maintain normal levels of several downstream osteogenic genes (Riddle et al., 2013). Since R-spondins are known to inhibit LRP internalization by RNF43/ZNRF3, it is consistent that Rspo2-null and Lrp5/6 null cells would have similar gene expression profiles.

The discordance between the osteogenic phenotypes of models of disruptions of osteogenic genes (such as Osterix) with our Rspo2 conditional knockout model invites the question of what other pathways, other than traditional beta-catenin signaling, may be involved in modulating the alternative osteogenic pathways. Given that R-spondins are known to modulate both canonical and noncanonical Wnt signaling, the noncanonical pathway is one likely potential alternative pathway. The furin domains of R-spondin are known to activate canonical Wnt signaling, while several reports have indicated that the TSR-1 domain activates noncanonical Wnt signaling (Kim et al., 2008; Ohkawara et al., 2011). To investigate this further, we generated domain-deletion constructs of Rspo2 for viral expression in MPC and analysis of osteogenesis (Figure 3.3). Initial findings show that full-length Rspo2 (WT) does not enhance mineralization in WT MPC compared to cells transduced with a control virus containing mCherry (mCh), similar to the treatment of WT MPC with recombinant RSPO2 in Chapter 2. However, full-length Rspo2 does increase the mineralization of Rspo2-null MPC. Rspo2 lacking the furin

63

domains (dFur) and Rspo2 lacking the TSR-1 domain (dTSR) both increase mineralization in WT and Rspo2-null MPC. However, Rspo2 lacking the region corresponding to exons 4 and 5 (dEx4-5, as in the conditional knockout model), appears to result in inhibition of mineralization in the WT MPC while increasing mineralization in Rspo2-null MPC (Figure 3.4). These data suggest that the furin and TSR domains may be acting in direct opposition to one another, as removal of either results in increased mineralization. The removal of one of the furin domains and the TSR-1 domain, as in dEx4-5, is more complex and likely involves interaction with endogenous full-length Rspo2 given the opposite effects in WT versus Rspo2-null MPC. If the domains are in fact working in opposition to one another, this may be consistent with the Furin domain enhancing canonical and the TSR enhancing noncanonical Wnt signaling. However, if that is the case, both canonical and noncanonical signaling would have to enhance osteoblastogenesis and mineralization, while also inhibiting the alternative type of Wnt signaling.

The role of non-canonical Wnt signaling in osteoblasts and bone biology remains poorly understood. As discussed in the previous chapters, a significant body of research supports that canonical Wnt signaling enhances osteoblastogenesis, though level of signaling through the pathway at various points in differentiation do not always produce a linear response. The data regarding the effects of noncanonical Wnt signaling are more variable. Explanations for this variability include: i) Wnt ligands are not as specific for canonical versus noncanonical as they were originally hypothesized, ii) there are many noncanonical signaling pathways in contrast to the singular canonical Wnt signaling pathway, and iii) due to the lack of pathway specific tools, it becomes more difficult to manipulate non-canonical signaling. To investigate this in our hands, we added small molecule inhibitors and activators of canonical Wnt/beta-catenin and noncanonical Wnt/PCP signaling in the media of differentiating cells. Though we had initially

64

hoped to do this in our Rspo2-null MPC, these cells proved too sensitive to survive functional

concentrations of the small molecules. However, we were able to test these constructs in

MC3T3-E1 pre-osteoblast cells. We found that lithium chloride (LiCl, a canonical Wnt signaling

agonist) did not cause noticeable changes in mineralization and ALP staining, as has been seen in

MC3T3-E1 cells previously. However, JNK-IN-8 (JI8, a Wnt/PCP signaling antagonist) increased

mineralization, while pyrvinium (Pyr, a canonical Wnt signaling antagonist) and anisomycin (Ani,

a Wnt/PCP signaling agonist) decreased mineralization and ALP staining in these cells (Figure

3.5). These data are consistent with canonical Wnt signaling supporting enhanced

osteoblastogenesis and noncanonical Wnt/PCP signaling inhibiting osteoblastogenesis. While

this is somewhat discordant with the preliminary Rspo2 domain deletion data above, it does

support much of the current literature, and it is possible that the TSR-1 domain is functioning

through a different noncanonical pathway, or even a different signaling pathway altogether.

Overall, our data support the role of Rspo2 as a potentiator of osteoblastogenesis and

define its role as necessary for normal osteoblastogenesis. Furthermore, the osteogenesis

defects of Rspo2-null MPC are most similar to the Lrp5- and Lrp6-null MPC, which is consistent

with their currently accepted interactions in modulation of canonical Wnt signaling.

R-Spondin-2 deficiency in osteoblasts causes defective mineralization and decreased bone

While it is important to investigate osteoblastogenesis in vitro, it is also fundamental to

examine osteoblastogenesis and osteoblast function in vivo. However, the global Rspo2[ftl]

knockout mouse is perinatal lethal, precluding the study of postnatal bone. These mice do form

bone in utero, unlike the Runx2- and Osx-knockout mice, but also have skeletogenesis defects

resulting from altered signaling at the apical ectodermal ridge (AER) of the developing limbs

65

(Bell et al., 2003; Bell et al., 2008). Limb histology of embryonic Rspo2-deficient mice revealed differences in the zones of endochondral ossification consistent with the published work on Rspo2 disruption effects on the growth plate, but did not reveal further information regarding mature bone (data not shown) (Takegami et al., 2016). To circumvent the problems of perinatal lethality in complete Rspo2-knockouts, we created a novel conditional Rspo2-knockout model. The model uses the Cre-Lox recombination system, with loxP sites inserted 5' and 3' of exons 4 and 5 of Rspo2. These exons correspond to one of the furin domains and the TSR-1 domain of Rspo2, which should produce a nonfunctional protein since it has been reported that both furin domains are needed in order to potentiate canonical Wnt signaling. This atypical targeting scheme was used because: i) the exons of Rspo2 are all in frame, ii) there is insufficient information about the endogenous Rspo2 promoter for targeting disruption of transcription, and iii) very large introns precluded targeting a larger region with homologous recombination. To confirm that this produced a non-functional Rspo2, this model was crossed to the EIIa-Cre mouse model for whole-body recombination with verified expression in bone. As reported in Chapter 2, homozygous targeted mice that were Cre-positive were all affected by skeletogenesis defects reminiscent of those seen in the global Rspo2^{ftl} model. On average, the defects were less severe than the Rspo2^{ftl} mouse, but this is to be expected in a Lox-Cre model as recombination is not 100% efficient.

We then crossed our new conditional Rspo2-knockout model to the Ocn-Cre model for specific Rspo2 knockout in osteoblasts, and we identified a mineralization defect that results in decreased bone mass. Interestingly, the model is most osteopenic at 3 months of age, with significantly less trabecular and cortical bone at this timepoint. At 6 months, the cortical bone geometry is no longer significantly different from WT mice and the trabecular bone differences

66

are attenuated, but mechanical function (bending strength) remains significantly decreased. In addition, it can be assumed, given the timing of Ocn expression, that the mice are similar until close to birth. Thus, over the first 3 months, the period of maximal bone accrual, the Rspo2-knockout mice have increasingly lower bone mass compared to WT littermates, and sometime after this point, this difference begins to attenuate. 3 months of age is known to correspond to the peak trabecular bone mass in mice, following a period where bone formation exceeds bone resorption; therefore, defects in bone formation may be particularly evident during this time. The lack of progressive osteopenia, and indeed an attenuating phenotype, suggests that bone resorption may be concurrently decreased. This is supported by the decreased TRAP staining seen in this model, and could be due to decreased RANK ligand or increased osteoprotegerin produced by the defective osteoblasts. This could be particularly relevant for the goal of utilizing R-spondins or their receptors as a potential therapeutic target, as one would expect increased bone formation to be coupled with increased bone resorption.

In the osteoblast-specific Rspo2-knockout, there is a more significant reduction in trabecular bone mass than cortical bone mass. Though this is somewhat surprising, it has also been reported with other alterations of Wnt signaling in mouse models. For instance, the Wnt10b alterations and treatment with LiCl result in changes only in the trabecular bone (Bennett et al., 2005; Clément-Lacroix et al., 2005; Bennett et al., 2007). Clearly, regulation of cortical and trabecular bone mass can be influenced independently and/or variably by the same factors. This can be at least partially attributed to trabecular surfaces being subject to remodeling, while periosteal surfaces primarily undergo modeling (Sims and Martin, 2014). It may also reflect variable canonical Wnt responsiveness of cells forming cortical bone relative to those forming trabecular bone.

67

In this Rspo2-knockout model, the primary cause of decreased bone mass appears to be defective osteoblasts that are unable to create bone matrix normally. This results in a decreased mineral apposition rate on the trabeculae, and thus thinner trabeculae. The fraction of the bone surface that is mineralizing, and the number of osteoblasts per bone surface, are not different from the WT mice. This further confirms that there is a lack of appropriate matrix deposition and mineralization, ultimately resulting in decreased bone formation rate and bone mass. Interestingly, while there appear to be adequate numbers of osteoblasts, when the progenitor population of the bone marrow of these mice are measured, there is a reduction in the total progenitor population, as well as a reduction in the percentage that are osteoprogenitors. While this does not appear to be the mechanism of decreased bone mass in this model, it may cause a more severe phenotype if these mice were ovarectomized or sustained fractures (Hadjiargyrou and O'Keefe, 2014).

3.3 LIMITATIONS AND FUTURE DIRECTIONS

Limitations

As mentioned above, loxP sites were inserted around exons 4 and 5 of Rspo2. This atypical targeting strategy results in the deletion of one of the furin domains and the TSR-1 domain. Despite out observations, the signaling sequence, first furin domain, and C-terminus are intact and could theoretically produce a protein product. However, western blot analysis with an antibody directed at the C-terminus showed a strong reduction in protein expression. Further studies measuring mRNA fragments from either the N- or C-terminus could further delineate if any product is made. Given the decreased detection of the C-terminus by western blot and the recapitulation of the global knockout when the model is crossed to a pan-expressing Cre, this is likely a minimal limitation of the study.

68

In this study, we utilized the Ocn-Cre recombinase mouse model for specific recombination in the osteoblasts. This is not an inducible Cre, and Ocn expression is established to begin at approximately E17 in the mouse. This means that part of the phenotype identified in these mice could be due to late prenatal and postnatal development. These prenatal changes may cause skeletal developmental alterations that are the primary cause of the skeletal phenotypic changes identified at later timepoints rather than due to true osteoblastic deficiencies. The use of an inducible osteoblast-specific cre, such as Ocn-Cre-ER^{T2}, would eliminate these potential embryonic developmental effects for more precise identification of postnatal bone remodeling changes. However, we measured the skeletal phenotypes of these mice at 3 timepoints, correlating to a juvenile age, a young adult with peak trabecular bone mass, and a mature adult. Evaluating not merely one individual timepoint, but the changes across significant murine life stages allows for interpretation of the adult remodeling phenotype, along with any phenotype that may be more purely developmental. Furthermore, Ocn-Cre is not exclusively expressed in osteoblasts. It is also expressed in hypertrophic chondrocytes, and anecdotal reports have purported expression in the brain (Personal Communication, Warman). While there is a decrease in the femur length at all ages assessed in the targeted mice, their growth plates appear normal, unlike the growth plates of global Rspo2-knockout mice. Likewise, other disruptions of Wnt signaling result in shortened bones.

In this study, we primarily compared Ocn-Cre+ and Ocn-Cre- mice, both with a Rspo2$^{f/f}$ genotype. Initially, we included mice that were wild-type and heterozygous at the Rspo2 locus as well, but concentrated on the homozygous targeted mice after preliminary investigations. The Ocn-Cre-Rspo2$^{f/f}$ mice were the smallest of the control mice, consistent with previous mouse model studies involving genetic manipulation. Given this, these mice would not

69

overestimate the differences between wild-type and targeted mice, and in fact may underestimate these differences. These mice are also the closest in background to the targeted mice, which is why they were selected for our complete studies. It is possible that the floxed allele alone could lead to differences in bone regulation that we did not control for. Since these were not seen in preliminary investigations, this limitation in our studies is likely minimal.

The mouse as a model for human bone is imperfect. Mice do not have Haversian systems in their cortical bone, thus they do not remodel their cortical bone in the same way that humans do. However, they do remodel their trabecular bone similarly to humans, albeit at a higher rate due to their higher overall metabolism. Additionally, mice do not have closure of their growth plates with the associated fusion of the metaphysis and epiphysis. However, growth slows significantly with sexual maturity, and in C57Bl/6 mice specifically, no further femoral lengthening has been observed past 6 months of age (Jilka, 2013). If Rspo2 was thought to play an important role in Haversian remodeling, another animal model would need to be utilized. There is a known mRNA-stabilizing mutation in Rspo2 in dogs that results in external changes visualized in their coats, but their bones have not yet been investigated (Cadieu et al., 2009). Given the easily identifiable external features of dogs with the mutation due to coat changes, and the extensively established pedigrees of purebred dogs, this would be an excellent model to identify cortical bone mass alterations in the context of alterations in Rspo2.

In this dissertation, only long bones were analyzed. Further investigation into the axial skeleton is warranted given the changes identified in the appendicular skeleton. Similarly, alterations in vertebral bone mass have been identified with alterations in Wnt signaling. Moreover, decreased bone mass in the vertebrae and resultant fractures are common in osteoporosis, making bone loss in this region particularly clinically significant. Our studies

establish changes in bone mass regulation in a mouse model, and these could be extended to the axial skeleton as well.

Finally, in our investigations of both MPC and BM-MSC, we are culturing a mixed population of cells. Though these populations are primarily progenitor and pre-osteoblast cells, there are a small percentage of cells that are of other types and could contribute to the phenotypes measured. Isolation of cells of both types is commonly used in many labs, though, so comparisons can be easily made. Purified populations of cells could be isolated based on cell-surface markers, but there is little consensus regarding which markers should be used for sorting MSC of mice. For the purposes of our studies, these populations of cells were considered of sufficiently pure quality, and we did not observe differences between the cells of any genotype via microscopy. Importantly, two distinct cell types deficient in Rspo2, embryonic limb bud and marrow-derived MSC from adults, showed a similar phenotype.

Future Directions

Elucidate the structure-function mechanism of Rspo2 activity

Our data show that Rspo2 is critical for normal osteoblastogenesis and bone accrual, and that addition of Rspo2 enhances these processes. We have preliminary data suggesting that the modular structure of Rspo2 may allow it to signal through multiple pathways, and that these functions may oppose each other during osteoblastogenesis. Continued investigation utilizing the domain-deletion mutants into the osteogenic gene expression and activity of potential signaling pathways will further elucidate this. Specifically, crossing this mouse line to a Wnt-reporter mouse line such as the TOPGAL mouse line, would elucidate changes in canonical Wnt signaling in mice with Rspo2-deficient osteoblasts. In vitro, this could also be investigated

71

transfecting Rspo2-deficient osteoblasts with a luciferase Wnt reporter such as TOPFlash and comparing light emission with WT osteoblasts. Increased understanding of Rspo2 mechanisms of action could potentially lead to greater enhancement of osteoblastogenesis and bone accrual, as well as provide a way to fine-tune the level of osteogenic stimulation to different levels as clinically appropriate.

Redundancy of R-spondins

The R-Spondins are a family of four similar molecules, as discussed in Chapter one. It is very likely that there is some redundancy between them. Creating compound knockouts, as well as measuring the expression of the other R-spondins in the context of knockdown of one family member are potential options for how this investigation could be pursued. So far it has been reported that conditional deletion of Rspo3 in developing limb mesenchyme of Rspo2 heterozygous mice increases the skeletogenesis defects (McGee-Lawrence et al., 2011).

Osteoblast-osteoclast coupling with Rspo2-deficient osteoblasts

Osteoblast-osteoclast coupling in vivo is well established, and is one of the primary mechanisms of regulation of bone mass. Here, we show that when Rspo2 is disrupted in osteoblasts, TRAP staining of osteoclasts decreases. This suggests that stimulation of osteoclasts by these defective osteoblasts also decreases. It would be informative to measure RANKL and osteoprotegerin expression in osteoblasts, as well as to study osteoclasts cultured in conditioned media from Rspo2-null osteoblasts. This coupling is an important consideration when selecting targets and designing novel therapeutics for the regulation of bone mass.

Rspo2-deficiency in models of low bone mass and regeneration

One of the most important next studies will be to challenge the mice with Rspo2 disruption in their osteoblasts. This can be done via ovariectomy or administration of corticosteroid, which result in loss of bone mass in mice. Disuse models via tail suspension can also be used for this purpose. Fracture studies could also be performed to investigate the regenerative ability of Rspo2-null osteoblasts. Of course, the reciprocal experiments of challenging the models using one of these mechanisms and adding Rspo2 would also be very informative regarding Rspo2's potential to aid in reducing osteoporotic bone loss and enhancing fracture healing.

3.4 CONCLUDING REMARKS

This dissertation is the first report of an Rspo2 conditional knockout mouse model, as well as being the first to investigate Rspo2 in postnatal bone. Specifically, mice with Rspo2-null osteoblasts were shown to have decreased bone mass due to defective osteoblasts. These osteoblasts lead to a decreased bone formation rate, thus causing the mice to have thinner trabeculae and reduced overall bone volume fraction. Mice with Rspo2-null osteoblasts also had fewer progenitor cells in their bone marrow. These findings were corroborated by decreased osteoblastogenesis and mineralization of Rspo2-null mesenchymal progenitor cells in vitro. These data establish Rspo2 as a critical regulator of bone mass for the first time. Development of this new mouse model provides the foundational steps for evaluation of Rspo2 function in osteoblasts during bone loss and fracture, and ultimately in establishing novel therapeutics for regulating bone mass based on the Wnt agonist Rspo2.
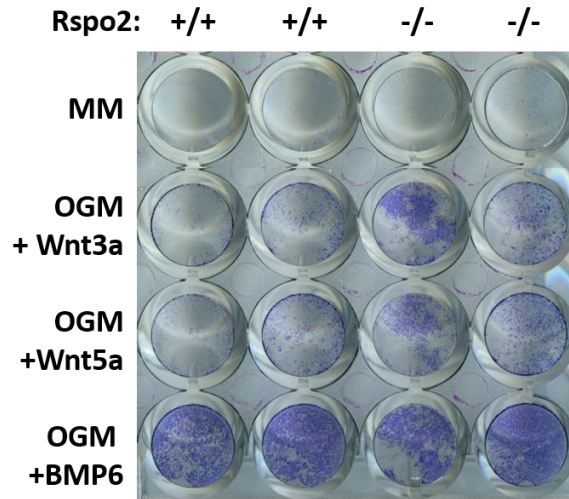
73

Figure 3.1. Alkaline Phosphatase staining of Rspo2-null MPC undergoing Wnt-stimulated osteoblastogenesis. Cells were treated with 100ng/mL Wnt3a, 100ng/mL Wnt5a, or 2.5nM BMP6. Staining at 7 days post-osteogenic induction. MM = Maintenance Media; OGM = Osteogenic Media.
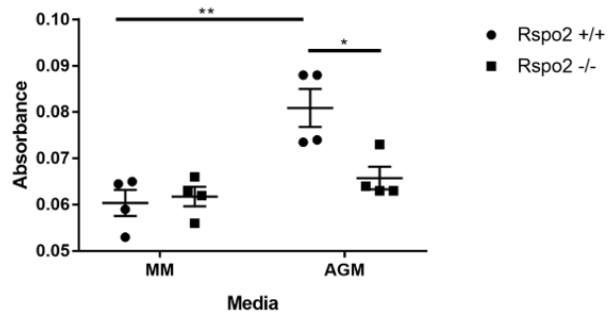
Figure 3.2. Rspo2-null MPC have reduced adipogenesis in vitro. Quantification of Oil Red O staining of wells 7 days post induction of adipogenesis. MM = Maintenance Media, AGM = Adipogenic Media. $*p<0.05$, $**p<0.01$ by 2-way ANOVA with Tukey's corrections for multiple comparisons.
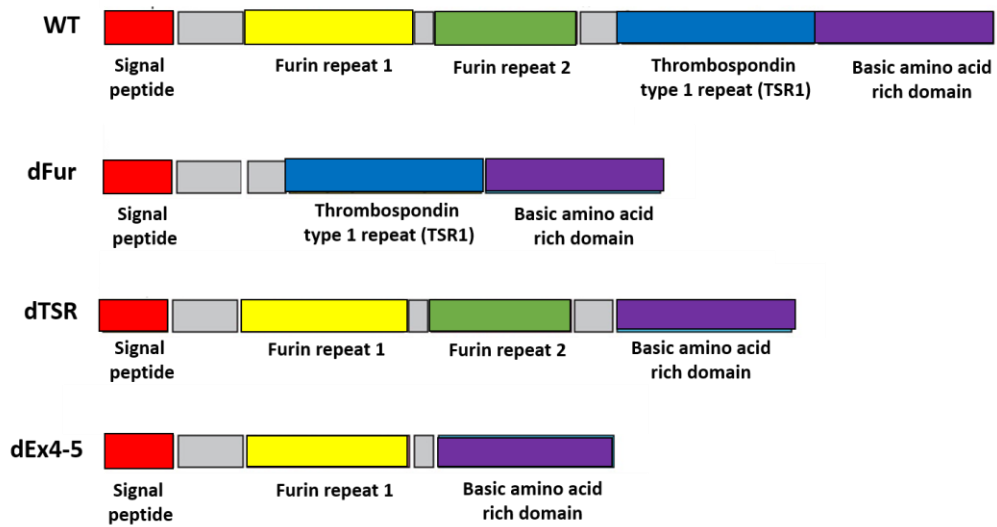
75

Figure 3.3. Rspo2 domain-deletion constructs. Domain-deletion constructs designed to test the structure-function relationship of Rspo2. dFur lacks both Furin repeat domains. dTSR lacks the Thrombospondin type 1 repeat domain. dEx4-5 lacks the region corresponding to Exons 4 and 5, similar to the conditional Rspo2-knockout mouse model.
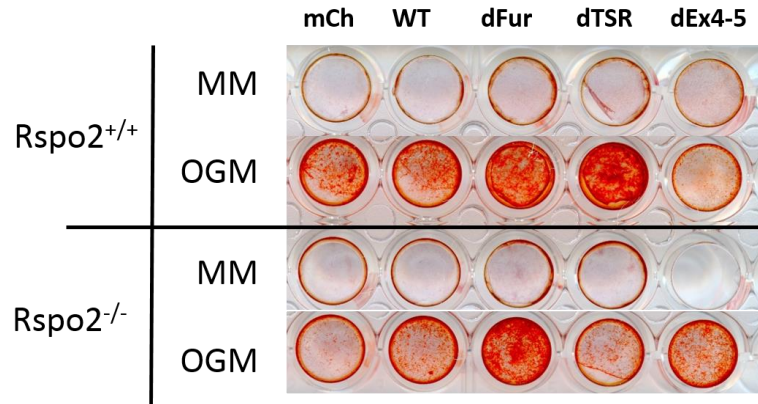
Figure 3.4. Osteogenesis of MPC with Rspo2 domain-deletion constructs. Alizarin red S staining of MPC 10 days post-induction of osteogenesis. Cells were transduced with lentivirus according to the indicated labels: mCh=mCherry, WT=full-length Rspo2, dFur=Rspo2 lacking the furin domains, dTSR=Rspo2 lacking the TSR-1 domain, dEx4-5=Rspo2 lacking the region corresponding to exons 4 and 5. MM = Maintenance Media, OGM = Osteogenic Media.

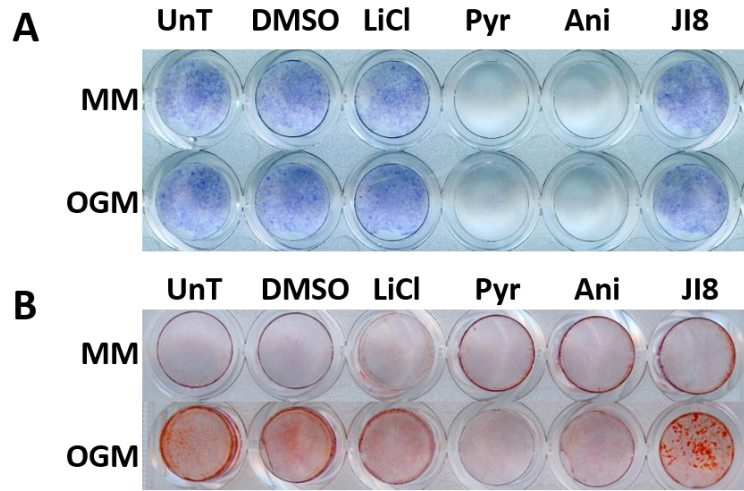**Figure 3.5. Osteogenesis of MC3T3-E1 cells treated with activators and inhibitors of Wnt signaling.** A. ALP staining of cells 5 days post induction of osteogenesis. B. Alizarin red S staining of mineralization of cells 10 days post induction of osteogenesis. MM = Maintenance Media, OGM = Osteogenic Media. UnT = Untreated, DMSO = vehicle control, LiCl = lithium chloride, Pyr = pyrvinium, Ani = Anisomycin, JI8 = JNK-Inhibitor-8.

BIBLIOGRAPHY

Abed, É, Chan, T. F., Delalandre, A., Martel-Pelletier, J., Pelletier, J. P. and Lajeunesse, D. (2011) 'R-spondins are newly recognized players in osteoarthritis that regulate Wnt signaling in osteoblasts', *Arthritis Rheum* 63(12): 3865-75.

Aoki, M., Kiyonari, H., Nakamura, H. and Okamoto, H. (2008) 'R-spondin2 expression in the apical ectodermal ridge is essential for outgrowth and patterning in mouse limb development', *Dev Growth Differ* 50(2): 85-95.

Aoki, M., Mieda, M., Ikeda, T., Hamada, Y., Nakamura, H. and Okamoto, H. (2007) 'R-spondin3 is required for mouse placental development', *Dev Biol* 301(1): 218-26.

Baenziger, N. L., Brodie, G. N. and Majerus, P. W. (1971) 'A thrombin-sensitive protein of human platelet membranes', *Proc Natl Acad Sci U S A* 68(1): 240-3.

Bahney, C. S., Hu, D. P., Taylor, A. J., Ferro, F., Britz, H. M., Hallgrimsson, B., Johnstone, B., Miclau, T. and Marcucio, R. S. (2014) 'Stem cell-derived endochondral cartilage stimulates bone healing by tissue transformation', *J Bone Miner Res* 29(5): 1269-82.

Baksh, D. and Tuan, R. S. (2007) 'Canonical and non-canonical Wnts differentially affect the development potential of primary isolate of human bone marrow mesenchymal stem cells', *J Cell Physiol* 212(3): 817-26.

Balemans, W., Patel, N., Ebeling, M., Van Hul, E., Wuyts, W., Lacza, C., Dioszegi, M., Dikkers, F. G., Hildering, P., Willems, P. J. et al. (2002) 'Identification of a 52 kb deletion downstream of the SOST gene in patients with van Buchem disease', *J Med Genet* 39(2): 91-7.

Bell, S. M., Schreiner, C. M., Hess, K. A., Anderson, K. P. and Scott, W. J. (2003) 'Asymmetric limb malformations in a new transgene insertional mutant, footless', *Mech Dev* 120(5): 597-605.

Bell, S. M., Schreiner, C. M., Wert, S. E., Mucenski, M. L., Scott, W. J. and Whitsett, J. A. (2008) 'R-spondin 2 is required for normal laryngeal-tracheal, lung and limb morphogenesis', *Development* 135(6): 1049-58.

Bell, T. D., Demay, M. B. and Burnett-Bowie, S. A. (2010) 'The biology and pathology of vitamin D control in bone', *J Cell Biochem* 111(1): 7-13.

Bennett, C. N., Longo, K. A., Wright, W. S., Suva, L. J., Lane, T. F., Hankenson, K. D. and MacDougald, O. A. (2005) 'Regulation of osteoblastogenesis and bone mass by Wnt10b', *Proc Natl Acad Sci U S A* 102(9): 3324-9.

Bennett, C. N., Ouyang, H., Ma, Y. L., Zeng, Q., Gerin, I., Sousa, K. M., Lane, T. F., Krishnan, V., Hankenson, K. D. and MacDougald, O. A. (2007) 'Wnt10b increases postnatal bone formation by enhancing osteoblast differentiation', *J Bone Miner Res* 22(12): 1924-32.

Bergmann, C., Senderek, J., Anhuf, D., Thiel, C. T., Ekici, A. B., Poblete-Gutierrez, P., van Steensel, M., Seelow, D., Nürnberg, G., Schild, H. H. et al. (2006) 'Mutations in the gene encoding the Wnt-signaling component R-spondin 4 (RSPO4) cause autosomal recessive anonychia', *Am J Hum Genet* 79(6): 1105-9.

Binnerts, M. E., Kim, K. A., Bright, J. M., Patel, S. M., Tran, K., Zhou, M., Leung, J. M., Liu, Y., Lomas, W. E., Dixon, M. et al. (2007) 'R-Spondin1 regulates Wnt signaling by inhibiting internalization of LRP6', *Proc Natl Acad Sci U S A* 104(37): 14700-5.

Bloomfield, S. A. (2010) 'Disuse osteopenia', *Curr Osteoporos Rep* 8(2): 91-7.

Bodenner, D., Redman, C. and Riggs, A. (2007) 'Teriparatide in the management of osteoporosis', *Clin Interv Aging* 2(4): 499-507.

Bonewald, L. F. (2011) 'The amazing osteocyte', *J Bone Miner Res* 26(2): 229-38.

Bouxsein, M. L., Boyd, S. K., Christiansen, B. A., Guldberg, R. E., Jepsen, K. J. and Müller, R. (2010) 'Guidelines for assessment of bone microstructure in rodents using micro-computed tomography', *J Bone Miner Res* 25(7): 1468-86.

Boyden, L. M., Mao, J., Belsky, J., Mitzner, L., Farhi, A., Mitnick, M. A., Wu, D., Insogna, K. and Lifton, R. P. (2002) 'High bone density due to a mutation in LDL-receptor-related protein 5', *N Engl J Med* 346(20): 1513-21.

Bruderer, M., Richards, R. G., Alini, M. and Stoddart, M. J. (2014) 'Role and regulation of RUNX2 in osteogenesis', *Eur Cell Mater* 28: 269-86.

Brunkow, M. E., Gardner, J. C., Van Ness, J., Paeper, B. W., Kovacevich, B. R., Proll, S., Skonier, J. E., Zhao, L., Sabo, P. J., Fu, Y. et al. (2001) 'Bone dysplasia sclerosteosis results from loss of the SOST gene product, a novel cystine knot-containing protein', *Am J Hum Genet* 68(3): 577-89.

Brüchle, N. O., Frank, J., Frank, V., Senderek, J., Akar, A., Koc, E., Rigopoulos, D., van Steensel, M., Zerres, K. and Bergmann, C. (2008) 'RSPO4 is the major gene in autosomal-recessive anonychia and mutations cluster in the furin-like cysteine-rich domains of the Wnt signaling ligand R-spondin 4', *J Invest Dermatol* 128(4): 791-6.

Burge, R., Dawson-Hughes, B., Solomon, D. H., Wong, J. B., King, A. and Tosteson, A. (2007) 'Incidence and economic burden of osteoporosis-related fractures in the United States, 2005-2025', *J Bone Miner Res* 22(3): 465-75.

Cadieu, E., Neff, M. W., Quignon, P., Walsh, K., Chase, K., Parker, H. G., Vonholdt, B. M., Rhue, A., Boyko, A., Byers, A. et al. (2009) 'Coat variation in the domestic dog is governed by variants in three genes', *Science* 326(5949): 150-3.

Carmon, K. S., Gong, X., Lin, Q., Thomas, A. and Liu, Q. (2011) 'R-spondins function as ligands of the orphan receptors LGR4 and LGR5 to regulate Wnt/beta-catenin signaling', *Proc Natl Acad Sci U S A* 108(28): 11452-7.

Caverzasio, Joseph (2009) 'Non-canonical Wnt signaling: What is its role in bone?', *IBMS BoneKEy* 6: 107-115.

Chadi, S., Buscara, L., Pechoux, C., Costa, J., Laubier, J., Chaboissier, M. C., Pailhoux, E., Vilotte, J. L., Chanat, E. and Le Provost, F. (2009) 'R-spondin1 is required for normal epithelial morphogenesis during mammary gland development', *Biochem Biophys Res Commun* 390(3): 1040-3.

Chen, J. Z., Wang, S., Tang, R., Yang, Q. S., Zhao, E., Chao, Y., Ying, K., Xie, Y. and Mao, Y. M. (2002) 'Cloning and identification of a cDNA that encodes a novel human protein with thrombospondin type I repeat domain, hPWTSR', *Mol Biol Rep* 29(3): 287-92.

Chen, P. H., Chen, X., Lin, Z., Fang, D. and He, X. (2013) 'The structural basis of R-spondin recognition by LGR5 and RNF43', *Genes Dev* 27(12): 1345-50.

Clarke, B. (2008) 'Normal bone anatomy and physiology', *Clin J Am Soc Nephrol* 3 Suppl 3: S131-9.

Clément-Lacroix, P., Ai, M., Morvan, F., Roman-Roman, S., Vayssière, B., Belleville, C., Estrera, K., Warman, M. L., Baron, R. and Rawadi, G. (2005) 'Lrp5-independent activation of Wnt signaling by lithium chloride increases bone formation and bone mass in mice', *Proc Natl Acad Sci U S A* 102(48): 17406-11.

Cruciat, C. M. and Niehrs, C. (2013) 'Secreted and transmembrane wnt inhibitors and activators', *Cold Spring Harb Perspect Biol* 5(3): a015081.

Cui, Y., Niziolek, P. J., MacDonald, B. T., Zylstra, C. R., Alenina, N., Robinson, D. R., Zhong, Z., Matthes, S., Jacobsen, C. M., Conlon, R. A. et al. (2011) 'Lrp5 functions in bone to regulate bone mass', *Nat Med* 17(6): 684-91.

Cummings, S. R., San Martin, J., McClung, M. R., Siris, E. S., Eastell, R., Reid, I. R., Delmas, P., Zoog, H. B., Austin, M., Wang, A. et al. (2009) 'Denosumab for prevention of fractures in postmenopausal women with osteoporosis', *N Engl J Med* 361(8): 756-65.

Day, T. F., Guo, X., Garrett-Beal, L. and Yang, Y. (2005) 'Wnt/beta-catenin signaling in mesenchymal progenitors controls osteoblast and chondrocyte differentiation during vertebrate skeletogenesis', *Dev Cell* 8(5): 739-50.

de Lau, W. B., Snel, B. and Clevers, H. C. (2012) 'The R-spondin protein family', *Genome Biol* 13(3): 242.

de Lau, W., Barker, N., Low, T. Y., Koo, B. K., Li, V. S., Teunissen, H., Kujala, P., Haegebarth, A., Peters, P. J., van de Wetering, M. et al. (2011) 'Lgr5 homologues associate with Wnt receptors and mediate R-spondin signalling', *Nature* 476(7360): 293-7.

Dempster, D. W., Compston, J. E., Drezner, M. K., Glorieux, F. H., Kanis, J. A., Malluche, H., Meunier, P. J., Ott, S. M., Recker, R. R. and Parfitt, A. M. (2013) 'Standardized nomenclature, symbols, and units for bone histomorphometry: a 2012 update of the report of the ASBMR Histomorphometry Nomenclature Committee', *J Bone Miner Res* 28(1): 2-17.

Dhanwal, D. K., Dennison, E. M., Harvey, N. C. and Cooper, C. (2011) 'Epidemiology of hip fracture: Worldwide geographic variation', *Indian J Orthop* 45(1): 15-22.

Fitzpatrick, L. A. (2002) 'Secondary causes of osteoporosis', *Mayo Clin Proc* 77(5): 453-68.

Florencio-Silva, R., Sasso, G. R., Sasso-Cerri, E., Simões, M. J. and Cerri, P. S. (2015) 'Biology of Bone Tissue: Structure, Function, and Factors That Influence Bone Cells', *Biomed Res Int* 2015: 421746.

Friedman, M. S., Oyserman, S. M. and Hankenson, K. D. (2009) 'Wnt11 promotes osteoblast maturation and mineralization through R-spondin 2', *J Biol Chem* 284(21): 14117-25.

Fujino, T., Asaba, H., Kang, M. J., Ikeda, Y., Sone, H., Takada, S., Kim, D. H., Ioka, R. X., Ono, M., Tomoyori, H. et al. (2003) 'Low-density lipoprotein receptor-related protein 5 (LRP5) is essential for normal cholesterol metabolism and glucose-induced insulin secretion', *Proc Natl Acad Sci U S A* 100(1): 229-34.

Fukumoto, S. and Matsumoto, T. (2017) 'Recent advances in the management of osteoporosis', *F1000Res* 6: 625.

Glass, D. A., Bialek, P., Ahn, J. D., Starbuck, M., Patel, M. S., Clevers, H., Taketo, M. M., Long, F., McMahon, A. P., Lang, R. A. et al. (2005) 'Canonical Wnt signaling in differentiated osteoblasts controls osteoclast differentiation', *Dev Cell* 8(5): 751-64.

Glinka, A., Dolde, C., Kirsch, N., Huang, Y. L., Kazanskaya, O., Ingelfinger, D., Boutros, M., Cruciat, C. M. and Niehrs, C. (2011) 'LGR4 and LGR5 are R-spondin receptors mediating Wnt/β-catenin and Wnt/PCP signalling', *EMBO Rep* 12(10): 1055-61.

Gong, Y., Slee, R. B., Fukai, N., Rawadi, G., Roman-Roman, S., Reginato, A. M., Wang, H., Cundy, T., Glorieux, F. H., Lev, D. et al. (2001) 'LDL receptor-related protein 5 (LRP5) affects bone accrual and eye development', *Cell* 107(4): 513-23.

Gregson, C. L., Steel, S. A., O'Rourke, K. P., Allan, K., Ayuk, J., Bhalla, A., Clunie, G., Crabtree, N., Fogelman, I., Goodby, A. et al. (2012) ''Sink or swim': an evaluation of the clinical characteristics of individuals with high bone mass', *Osteoporos Int* 23(2): 643-54.

Hadjiargyrou, M. and O'Keefe, R. J. (2014) 'The convergence of fracture repair and stem cells: interplay of genes, aging, environmental factors and disease', *J Bone Miner Res* 29(11): 2307-22.

Hankenson, K. D., Sweetwyne, M. T., Shitaye, H. and Posey, K. L. (2010) 'Thrombospondins and novel TSR-containing proteins, R-spondins, regulate bone formation and remodeling', *Curr Osteoporos Rep* 8(2): 68-76.

Hao, H. X., Xie, Y., Zhang, Y., Charlat, O., Oster, E., Avello, M., Lei, H., Mickanin, C., Liu, D., Ruffner, H. et al. (2012) 'ZNRF3 promotes Wnt receptor turnover in an R-spondin-sensitive manner', *Nature* 485(7397): 195-200.

Harada, S. and Rodan, G. A. (2003) 'Control of osteoblast function and regulation of bone mass', *Nature* 423(6937): 349-55.

Hill, T. P., Später, D., Taketo, M. M., Birchmeier, W. and Hartmann, C. (2005) 'Canonical Wnt/beta-catenin signaling prevents osteoblasts from differentiating into chondrocytes', *Dev Cell* 8(5): 727-38.

Holmen, S. L., Giambernardi, T. A., Zylstra, C. R., Buckner-Berghuis, B. D., Resau, J. H., Hess, J. F., Glatt, V., Bouxsein, M. L., Ai, M., Warman, M. L. et al. (2004) 'Decreased BMD and limb deformities in mice carrying mutations in both Lrp5 and Lrp6', *J Bone Miner Res* 19(12): 2033-40.

Holmen, S. L., Zylstra, C. R., Mukherjee, A., Sigler, R. E., Faugere, M. C., Bouxsein, M. L., Deng, L., Clemens, T. L. and Williams, B. O. (2005) 'Essential role of beta-catenin in postnatal bone acquisition', *J Biol Chem* 280(22): 21162-8.

Hu, H., Hilton, M. J., Tu, X., Yu, K., Ornitz, D. M. and Long, F. (2005) 'Sequential roles of Hedgehog and Wnt signaling in osteoblast development', *Development* 132(1): 49-60.

Jilka, R. L. (2013) 'The relevance of mouse models for investigating age-related bone loss in humans', *J Gerontol A Biol Sci Med Sci* 68(10): 1209-17.

Johnell, O. and Kanis, J. A. (2006) 'An estimate of the worldwide prevalence and disability associated with osteoporotic fractures', *Osteoporos Int* 17(12): 1726-33.

Kamata, T., Katsube, K., Michikawa, M., Yamada, M., Takada, S. and Mizusawa, H. (2004) 'R-spondin, a novel gene with thrombospondin type 1 domain, was expressed in the dorsal neural tube and affected in Wnts mutants', *Biochim Biophys Acta* 1676(1): 51-62.

Kanis, J. A. (1994) 'Assessment of fracture risk and its application to screening for postmenopausal osteoporosis: synopsis of a WHO report. WHO Study Group', *Osteoporos Int* 4(6): 368-81.

Kanis, J. A. (2002) 'Diagnosis of osteoporosis and assessment of fracture risk', *Lancet* 359(9321): 1929-36.

Kanis, J. A., Melton, L. J., Christiansen, C., Johnston, C. C. and Khaltaev, N. (1994) 'The diagnosis of osteoporosis', *J Bone Miner Res* 9(8): 1137-41.

Karasik, D., Rivadeneira, F. and Johnson, M. L. (2016) 'The genetics of bone mass and susceptibility to bone diseases', *Nat Rev Rheumatol* 12(6): 323-34.

Kato, M., Patel, M. S., Levasseur, R., Lobov, I., Chang, B. H., Glass, D. A., Hartmann, C., Li, L., Hwang, T. H., Brayton, C. F. et al. (2002) 'Cbfa1-independent decrease in osteoblast proliferation, osteopenia, and persistent embryonic eye vascularization in mice deficient in Lrp5, a Wnt coreceptor', *J Cell Biol* 157(2): 303-14.

Kazanskaya, O., Glinka, A., del Barco Barrantes, I., Stannek, P., Niehrs, C. and Wu, W. (2004) 'R-Spondin2 is a secreted activator of Wnt/beta-catenin signaling and is required for Xenopus myogenesis', *Dev Cell* 7(4): 525-34.

Kazanskaya, O., Ohkawara, B., Heroult, M., Wu, W., Maltry, N., Augustin, H. G. and Niehrs, C. (2008) 'The Wnt signaling regulator R-spondin 3 promotes angioblast and vascular development', *Development* 135(22): 3655-64.

Keats, E. C., Dominguez, J. M., Grant, M. B. and Khan, Z. A. (2014) 'Switch from canonical to noncanonical Wnt signaling mediates high glucose-induced adipogenesis', *Stem Cells* 32(6): 1649-60.

Kennell, J. A. and MacDougald, O. A. (2005) 'Wnt signaling inhibits adipogenesis through beta-catenin-dependent and -independent mechanisms', *J Biol Chem* 280(25): 24004-10.

Kim, J. A., Choi, H. K., Kim, T. M., Leem, S. H. and Oh, I. H. (2015) 'Regulation of mesenchymal stromal cells through fine tuning of canonical Wnt signaling', *Stem Cell Res* 14(3): 356-68.

Kim, K. A., Kakitani, M., Zhao, J., Oshima, T., Tang, T., Binnerts, M., Liu, Y., Boyle, B., Park, E., Emtage, P. et al. (2005) 'Mitogenic influence of human R-spondin1 on the intestinal epithelium', *Science* 309(5738): 1256-9.

Kim, K. A., Wagle, M., Tran, K., Zhan, X., Dixon, M. A., Liu, S., Gros, D., Korver, W., Yonkovich, S., Tomasevic, N. et al. (2008) 'R-Spondin family members regulate the Wnt pathway by a common mechanism', *Mol Biol Cell* 19(6): 2588-96.

Kim, K. A., Zhao, J., Andarmani, S., Kakitani, M., Oshima, T., Binnerts, M. E., Abo, A., Tomizuka, K. and Funk, W. D. (2006) 'R-Spondin proteins: a novel link to beta-catenin activation', *Cell Cycle* 5(1): 23-6.

Knight, M. N. and Hankenson, K. D. (2013) 'Mesenchymal Stem Cells in Bone Regeneration', *Adv Wound Care (New Rochelle)* 2(6): 306-316.

Knight, M. N. and Hankenson, K. D. (2014) 'R-spondins: Novel matricellular regulators of the skeleton', *Matrix Biol* 37C: 157-161.

Kobayashi, Y., Uehara, S., Koide, M. and Takahashi, N. (2015) 'The regulation of osteoclast differentiation by Wnt signals', *Bonekey Rep* 4: 713.

Kobayashi, Y., Uehara, S., Udagawa, N. and Takahashi, N. (2016) 'Regulation of bone metabolism by Wnt signals', *J Biochem* 159(4): 387-92.

Koo, B. K., Spit, M., Jordens, I., Low, T. Y., Stange, D. E., van de Wetering, M., van Es, J. H., Mohammed, S., Heck, A. J., Maurice, M. M. et al. (2012) 'Tumour suppressor RNF43 is a stem-cell E3 ligase that induces endocytosis of Wnt receptors', *Nature* 488(7413): 665-9.

Kramer, I., Halleux, C., Keller, H., Pegurri, M., Gooi, J. H., Weber, P. B., Feng, J. Q., Bonewald, L. F. and Kneissel, M. (2010) 'Osteocyte Wnt/beta-catenin signaling is required for normal bone homeostasis', *Mol Cell Biol* 30(12): 3071-85.

Krause, C., Korchynskyi, O., de Rooij, K., Weidauer, S. E., de Gorter, D. J., van Bezooijen, R. L., Hatsell, S., Economides, A. N., Mueller, T. D., Löwik, C. W. et al. (2010) 'Distinct modes of inhibition by sclerostin on bone morphogenetic protein and Wnt signaling pathways', *J Biol Chem* 285(53): 41614-26.

Krönke, G., Uderhardt, S., Kim, K. A., Stock, M., Scholtysek, C., Zaiss, M. M., Surmann-Schmitt, C., Luther, J., Katzenbeisser, J., David, J. P. et al. (2010) 'R-spondin 1 protects against inflammatory bone damage during murine arthritis by modulating the Wnt pathway', *Arthritis Rheum* 62(8): 2303-12.

Kugimiya, F., Kawaguchi, H., Ohba, S., Kawamura, N., Hirata, M., Chikuda, H., Azuma, Y., Woodgett, J. R., Nakamura, K. and Chung, U. I. (2007) 'GSK-3beta controls osteogenesis through regulating Runx2 activity', *PLoS One* 2(9): e837.

Lakso, M., Pichel, J. G., Gorman, J. R., Sauer, B., Okamoto, Y., Lee, E., Alt, F. W. and Westphal, H. (1996) 'Efficient in vivo manipulation of mouse genomic sequences at the zygote stage', *Proc Natl Acad Sci U S A* 93(12): 5860-5.

Langdahl, B., Ferrari, S. and Dempster, D. W. (2016) 'Bone modeling and remodeling: potential as therapeutic targets for the treatment of osteoporosis', *Ther Adv Musculoskelet Dis* 8(6): 225-235.

Lim, S. Y. and Bolster, M. B. (2017) 'Profile of romosozumab and its potential in the management of osteoporosis', *Drug Des Devel Ther* 11: 1221-1231.

Lin, G. L. and Hankenson, K. D. (2011) 'Integration of BMP, Wnt, and notch signaling pathways in osteoblast differentiation', *J Cell Biochem* 112(12): 3491-501.

Little, R. D., Carulli, J. P., Del Mastro, R. G., Dupuis, J., Osborne, M., Folz, C., Manning, S. P., Swain, P. M., Zhao, S. C., Eustace, B. et al. (2002) 'A mutation in the LDL receptor-related protein 5 gene results in the autosomal dominant high-bone-mass trait', *Am J Hum Genet* 70(1): 11-9.

Lu, W., Kim, K. A., Liu, J., Abo, A., Feng, X., Cao, X. and Li, Y. (2008) 'R-spondin1 synergizes with Wnt3A in inducing osteoblast differentiation and osteoprotegerin expression', *FEBS Lett* 582(5): 643-50.

Luo, J., Zhou, W., Zhou, X., Li, D., Weng, J., Yi, Z., Cho, S. G., Li, C., Yi, T., Wu, X. et al. (2009) 'Regulation of bone formation and remodeling by G-protein-coupled receptor 48', *Development* 136(16): 2747-56.

Manolagas, S. C. (2000) 'Birth and death of bone cells: basic regulatory mechanisms and implications for the pathogenesis and treatment of osteoporosis', *Endocr Rev* 21(2): 115-37.

McClung, M. R., Grauer, A., Boonen, S., Bolognese, M. A., Brown, J. P., Diez-Perez, A., Langdahl, B. L., Reginster, J. Y., Zanchetta, J. R., Wasserman, S. M. et al. (2014) 'Romosozumab in Postmenopausal Women with Low Bone Mineral Density', *N Engl J Med*.

McGee-Lawrence, M. E., McCleary-Wheeler, A. L., Secreto, F. J., Razidlo, D. F., Zhang, M., Stensgard, B. A., Li, X., Stein, G. S., Lian, J. B. and Westendorf, J. J. (2011) 'Suberoylanilide hydroxamic acid (SAHA; vorinostat) causes bone loss by inhibiting immature osteoblasts', *Bone* 48(5): 1117-26.

Miclea, R. L., Karperien, M., Bosch, C. A., van der Horst, G., van der Valk, M. A., Kobayashi, T., Kronenberg, H. M., Rawadi, G., Akçakaya, P., Löwik, C. W. et al. (2009) 'Adenomatous polyposis coli-mediated control of beta-catenin is essential for both chondrogenic and osteogenic differentiation of skeletal precursors', *BMC Dev Biol* 9: 26.

Monroe, D. G., McGee-Lawrence, M. E., Oursler, M. J. and Westendorf, J. J. (2012) 'Update on Wnt signaling in bone cell biology and bone disease', *Gene* 492(1): 1-18.

Morvan, F., Boulukos, K., Clément-Lacroix, P., Roman Roman, S., Suc-Royer, I., Vayssière, B., Ammann, P., Martin, P., Pinho, S., Pognonec, P. et al. (2006) 'Deletion of a single allele of the Dkk1 gene leads to an increase in bone formation and bone mass', *J Bone Miner Res* 21(6): 934-45.

Nakashima, K., Zhou, X., Kunkel, G., Zhang, Z., Deng, J. M., Behringer, R. R. and de Crombrugghe, B. (2002) 'The novel zinc finger-containing transcription factor osterix is required for osteoblast differentiation and bone formation', *Cell* 108(1): 17-29.

Nam, J. S., Park, E., Turcotte, T. J., Palencia, S., Zhan, X., Lee, J., Yun, K., Funk, W. D. and Yoon, J. K. (2007a) 'Mouse R-spondin2 is required for apical ectodermal ridge maintenance in the hindlimb', *Dev Biol* 311(1): 124-35.

Nam, J. S., Turcotte, T. J., Smith, P. F., Choi, S. and Yoon, J. K. (2006) 'Mouse cristin/R-spondin family proteins are novel ligands for the Frizzled 8 and LRP6 receptors and activate beta-catenin-dependent gene expression', *J Biol Chem* 281(19): 13247-57.

Nam, J. S., Turcotte, T. J. and Yoon, J. K. (2007b) 'Dynamic expression of R-spondin family genes in mouse development', *Gene Expr Patterns* 7(3): 306-12.

Neufeld, S., Rosin, J. M., Ambasta, A., Hui, K., Shaneman, V., Crowder, R., Vickerman, L. and Cobb, J. (2012) 'A conditional allele of Rspo3 reveals redundant function of R-spondins during mouse limb development', *Genesis* 50(10): 741-9.

Nishimura, R., Wakabayashi, M., Hata, K., Matsubara, T., Honma, S., Wakisaka, S., Kiyonari, H., Shioi, G., Yamaguchi, A., Tsumaki, N. et al. (2012) 'Osterix regulates calcification and degradation

of chondrogenic matrices through matrix metalloproteinase 13 (MMP13) expression in association with transcription factor Runx2 during endochondral ossification', *J Biol Chem* 287(40): 33179-90.

Nusse, R. and Clevers, H. (2017) 'Wnt/β-Catenin Signaling, Disease, and Emerging Therapeutic Modalities', *Cell* 169(6): 985-999.

Ohkawara, B., Glinka, A. and Niehrs, C. (2011) 'Rspo3 binds syndecan 4 and induces Wnt/PCP signaling via clathrin-mediated endocytosis to promote morphogenesis', *Dev Cell* 20(3): 303-14.

Ominsky, M. S., Vlasseros, F., Jolette, J., Smith, S. Y., Stouch, B., Doellgast, G., Gong, J., Gao, Y., Cao, J., Graham, K. et al. (2010) 'Two doses of sclerostin antibody in cynomolgus monkeys increases bone formation, bone mineral density, and bone strength', *J Bone Miner Res* 25(5): 948-59.

Otto, F., Thornell, A. P., Crompton, T., Denzel, A., Gilmour, K. C., Rosewell, I. R., Stamp, G. W., Beddington, R. S., Mundlos, S., Olsen, B. R. et al. (1997) 'Cbfa1, a candidate gene for cleidocranial dysplasia syndrome, is essential for osteoblast differentiation and bone development', *Cell* 89(5): 765-71.

Padhi, D., Jang, G., Stouch, B., Fang, L. and Posvar, E. (2011) 'Single-dose, placebo-controlled, randomized study of AMG 785, a sclerostin monoclonal antibody', *J Bone Miner Res* 26(1): 19-26.

Panday, K., Gona, A. and Humphrey, M. B. (2014) 'Medication-induced osteoporosis: screening and treatment strategies', *Ther Adv Musculoskelet Dis* 6(5): 185-202.

Parker, H. G., Chase, K., Cadieu, E., Lark, K. G. and Ostrander, E. A. (2010) 'An insertion in the RSPO2 gene correlates with improper coat in the Portuguese water dog', *J Hered* 101(5): 612-7.

Parma, P., Radi, O., Vidal, V., Chaboissier, M. C., Dellambra, E., Valentini, S., Guerra, L., Schedl, A. and Camerino, G. (2006) 'R-spondin1 is essential in sex determination, skin differentiation and malignancy', *Nat Genet* 38(11): 1304-9.

Pinson, K. I., Brennan, J., Monkley, S., Avery, B. J. and Skarnes, W. C. (2000) 'An LDL-receptor-related protein mediates Wnt signalling in mice', *Nature* 407(6803): 535-8.

Radius Health, Inc. (2017) FDA Approves Radius Health's TYMLOS™ (abaloparatide), a Bone Building Agent for the Treatment of Postmenopausal Women with Osteoporosis at High Risk for Fracture.

Riddle, R. C., Diegel, C. R., Leslie, J. M., Van Koevering, K. K., Faugere, M. C., Clemens, T. L. and Williams, B. O. (2013) 'Lrp5 and Lrp6 exert overlapping functions in osteoblasts during postnatal bone acquisition', *PLoS One* 8(5): e63323.

Rigueur, D. and Lyons, K. M. (2014) 'Whole-mount skeletal staining', *Methods Mol Biol* 1130: 113-121.

Ruffner, H., Sprunger, J., Charlat, O., Leighton-Davies, J., Grosshans, B., Salathe, A., Zietzling, S., Beck, V., Therier, M., Isken, A. et al. (2012) 'R-Spondin potentiates Wnt/β-catenin signaling through orphan receptors LGR4 and LGR5', *PLoS One* 7(7): e40976.

Sharma, A. R., Choi, B. S., Park, J. M., Lee, D. H., Lee, J. E., Kim, H. S., Yoon, J. K., Song, D. K., Nam, J. S. and Lee, S. S. (2013) 'Rspo 1 promotes osteoblast differentiation via Wnt signaling pathway', *Indian J Biochem Biophys* 50(1): 19-25.

Sims, Natalie A and **Martin,** T   John (2014) 'Coupling the activities of bone formation and resorption: a multitude of signals within the basic multicellular unit', *BoneKEy Reports* 3.

Stevens, J. R., Miranda-Carboni, G. A., Singer, M. A., Brugger, S. M., Lyons, K. M. and Lane, T. F. (2010) 'Wnt10b deficiency results in age-dependent loss of bone mass and progressive reduction of mesenchymal progenitor cells', *J Bone Miner Res* 25(10): 2138-47.

Takada, I., Mihara, M., Suzawa, M., Ohtake, F., Kobayashi, S., Igarashi, M., Youn, M. Y., Takeyama, K., Nakamura, T., Mezaki, Y. et al. (2007) 'A histone lysine methyltransferase activated by non-canonical Wnt signalling suppresses PPAR-gamma transactivation', *Nat Cell Biol* 9(11): 1273-85.

Takegami, Y., Ohkawara, B., Ito, M., Masuda, A., Nakashima, H., Ishiguro, N. and Ohno, K. (2016) 'R-spondin 2 facilitates differentiation of proliferating chondrocytes into hypertrophic chondrocytes by enhancing Wnt/β-catenin signaling in endochondral ossification', *Biochem Biophys Res Commun* 473(1): 255-64.

Thirunavukkarasu, K., Halladay, D. L., Miles, R. R., Geringer, C. D. and Onyia, J. E. (2002) 'Analysis of regulator of G-protein signaling-2 (RGS-2) expression and function in osteoblastic cells', *J Cell Biochem* 85(4): 837-50.

Tomizuka, K., Horikoshi, K., Kitada, R., Sugawara, Y., Iba, Y., Kojima, A., Yoshitome, A., Yamawaki, K., Amagai, M., Inoue, A. et al. (2008) 'R-spondin1 plays an essential role in ovarian development through positively regulating Wnt-4 signaling', *Hum Mol Genet* 17(9): 1278-91.

Tuchendler, D. and Bolanowski, M. (2014) 'The influence of thyroid dysfunction on bone metabolism', *Thyroid Res* 7(1): 12.

Wang, H., Brennan, T. A., Russell, E., Kim, J. H., Egan, K. P., Chen, Q., Israelite, C., Schultz, D. C., Johnson, F. B. and Pignolo, R. J. (2013) 'R-Spondin 1 promotes vibration-induced bone formation in mouse models of osteoporosis', *J Mol Med (Berl)* 91(12): 1421-9.

Wei, Q., Yokota, C., Semenov, M. V., Doble, B., Woodgett, J. and He, X. (2007) 'R-spondin1 is a high affinity ligand for LRP6 and induces LRP6 phosphorylation and beta-catenin signaling', *J Biol Chem* 282(21): 15903-11.

Wei, W., Zeve, D., Suh, J. M., Wang, X., Du, Y., Zerwekh, J. E., Dechow, P. C., Graff, J. M. and Wan, Y. (2011) 'Biphasic and dosage-dependent regulation of osteoclastogenesis by β-catenin', *Mol Cell Biol* 31(23): 4706-19.

Yamada, W., Nagao, K., Horikoshi, K., Fujikura, A., Ikeda, E., Inagaki, Y., Kakitani, M., Tomizuka, K., Miyazaki, H., Suda, T. et al. (2009) 'Craniofacial malformation in R-spondin2 knockout mice', *Biochem Biophys Res Commun* 381(3): 453-8.

Zhang, L., Su, P., Xu, C., Chen, C., Liang, A., Du, K., Peng, Y. and Huang, D. (2010) 'Melatonin inhibits adipogenesis and enhances osteogenesis of human mesenchymal stem cells by suppressing PPARγ expression and enhancing Runx2 expression', *J Pineal Res* 49(4): 364-72.

Zhang, M., Xuan, S., Bouxsein, M. L., von Stechow, D., Akeno, N., Faugere, M. C., Malluche, H., Zhao, G., Rosen, C. J., Efstratiadis, A. et al. (2002) 'Osteoblast-specific knockout of the insulin-like growth factor (IGF) receptor gene reveals an essential role of IGF signaling in bone matrix mineralization', *J Biol Chem* 277(46): 44005-12.

Zhou, X., von der Mark, K., Henry, S., Norton, W., Adams, H. and de Crombrugghe, B. (2014) 'Chondrocytes transdifferentiate into osteoblasts in endochondral bone during development, postnatal growth and fracture healing in mice', *PLoS Genet* 10(12): e1004820.

Zuo, C., Huang, Y., Bajis, R., Sahih, M., Li, Y. P., Dai, K. and Zhang, X. (2012) 'Osteoblastogenesis regulation signals in bone remodeling', *Osteoporos Int* 23(6): 1653-63.